Safety Reports Series

No. 89

Diffuse Seismicity in Seismic Hazard Assessment for Site Evaluation of Nuclear Installations

IAEA
International Atomic Energy Agency

IAEA SAFETY STANDARDS AND RELATED PUBLICATIONS

IAEA SAFETY STANDARDS

Under the terms of Article III of its Statute, the IAEA is authorized to establish or adopt standards of safety for protection of health and minimization of danger to life and property, and to provide for the application of these standards.

The publications by means of which the IAEA establishes standards are issued in the **IAEA Safety Standards Series**. This series covers nuclear safety, radiation safety, transport safety and waste safety. The publication categories in the series are **Safety Fundamentals**, **Safety Requirements** and **Safety Guides**.

Information on the IAEA's safety standards programme is available on the IAEA Internet site

http://www-ns.iaea.org/standards/

The site provides the texts in English of published and draft safety standards. The texts of safety standards issued in Arabic, Chinese, French, Russian and Spanish, the IAEA Safety Glossary and a status report for safety standards under development are also available. For further information, please contact the IAEA at: Vienna International Centre, PO Box 100, 1400 Vienna, Austria.

All users of IAEA safety standards are invited to inform the IAEA of experience in their use (e.g. as a basis for national regulations, for safety reviews and for training courses) for the purpose of ensuring that they continue to meet users' needs. Information may be provided via the IAEA Internet site or by post, as above, or by email to Official.Mail@iaea.org.

RELATED PUBLICATIONS

The IAEA provides for the application of the standards and, under the terms of Articles III and VIII.C of its Statute, makes available and fosters the exchange of information relating to peaceful nuclear activities and serves as an intermediary among its Member States for this purpose.

Reports on safety in nuclear activities are issued as **Safety Reports**, which provide practical examples and detailed methods that can be used in support of the safety standards.

Other safety related IAEA publications are issued as **Emergency Preparedness and Response** publications, **Radiological Assessment Reports**, the International Nuclear Safety Group's **INSAG Reports**, **Technical Reports** and **TECDOCs**. The IAEA also issues reports on radiological accidents, training manuals and practical manuals, and other special safety related publications.

Security related publications are issued in the **IAEA Nuclear Security Series**.

The **IAEA Nuclear Energy Series** comprises informational publications to encourage and assist research on, and the development and practical application of, nuclear energy for peaceful purposes. It includes reports and guides on the status of and advances in technology, and on experience, good practices and practical examples in the areas of nuclear power, the nuclear fuel cycle, radioactive waste management and decommissioning.

DIFFUSE SEISMICITY IN SEISMIC HAZARD ASSESSMENT FOR SITE EVALUATION OF NUCLEAR INSTALLATIONS

The following States are Members of the International Atomic Energy Agency:

AFGHANISTAN
ALBANIA
ALGERIA
ANGOLA
ANTIGUA AND BARBUDA
ARGENTINA
ARMENIA
AUSTRALIA
AUSTRIA
AZERBAIJAN
BAHAMAS
BAHRAIN
BANGLADESH
BARBADOS
BELARUS
BELGIUM
BELIZE
BENIN
BOLIVIA, PLURINATIONAL STATE OF
BOSNIA AND HERZEGOVINA
BOTSWANA
BRAZIL
BRUNEI DARUSSALAM
BULGARIA
BURKINA FASO
BURUNDI
CAMBODIA
CAMEROON
CANADA
CENTRAL AFRICAN REPUBLIC
CHAD
CHILE
CHINA
COLOMBIA
CONGO
COSTA RICA
CÔTE D'IVOIRE
CROATIA
CUBA
CYPRUS
CZECH REPUBLIC
DEMOCRATIC REPUBLIC OF THE CONGO
DENMARK
DJIBOUTI
DOMINICA
DOMINICAN REPUBLIC
ECUADOR
EGYPT
EL SALVADOR
ERITREA
ESTONIA
ETHIOPIA
FIJI
FINLAND
FRANCE
GABON
GEORGIA
GERMANY
GHANA
GREECE
GUATEMALA
GUYANA
HAITI
HOLY SEE
HONDURAS
HUNGARY
ICELAND
INDIA
INDONESIA
IRAN, ISLAMIC REPUBLIC OF
IRAQ
IRELAND
ISRAEL
ITALY
JAMAICA
JAPAN
JORDAN
KAZAKHSTAN
KENYA
KOREA, REPUBLIC OF
KUWAIT
KYRGYZSTAN
LAO PEOPLE'S DEMOCRATIC REPUBLIC
LATVIA
LEBANON
LESOTHO
LIBERIA
LIBYA
LIECHTENSTEIN
LITHUANIA
LUXEMBOURG
MADAGASCAR
MALAWI
MALAYSIA
MALI
MALTA
MARSHALL ISLANDS
MAURITANIA
MAURITIUS
MEXICO
MONACO
MONGOLIA
MONTENEGRO
MOROCCO
MOZAMBIQUE
MYANMAR
NAMIBIA
NEPAL
NETHERLANDS
NEW ZEALAND
NICARAGUA
NIGER
NIGERIA
NORWAY
OMAN
PAKISTAN
PALAU
PANAMA
PAPUA NEW GUINEA
PARAGUAY
PERU
PHILIPPINES
POLAND
PORTUGAL
QATAR
REPUBLIC OF MOLDOVA
ROMANIA
RUSSIAN FEDERATION
RWANDA
SAN MARINO
SAUDI ARABIA
SENEGAL
SERBIA
SEYCHELLES
SIERRA LEONE
SINGAPORE
SLOVAKIA
SLOVENIA
SOUTH AFRICA
SPAIN
SRI LANKA
SUDAN
SWAZILAND
SWEDEN
SWITZERLAND
SYRIAN ARAB REPUBLIC
TAJIKISTAN
THAILAND
THE FORMER YUGOSLAV REPUBLIC OF MACEDONIA
TOGO
TRINIDAD AND TOBAGO
TUNISIA
TURKEY
TURKMENISTAN
UGANDA
UKRAINE
UNITED ARAB EMIRATES
UNITED KINGDOM OF GREAT BRITAIN AND NORTHERN IRELAND
UNITED REPUBLIC OF TANZANIA
UNITED STATES OF AMERICA
URUGUAY
UZBEKISTAN
VANUATU
VENEZUELA, BOLIVARIAN REPUBLIC OF
VIET NAM
YEMEN
ZAMBIA
ZIMBABWE

The Agency's Statute was approved on 23 October 1956 by the Conference on the Statute of the IAEA held at United Nations Headquarters, New York; it entered into force on 29 July 1957. The Headquarters of the Agency are situated in Vienna. Its principal objective is "to accelerate and enlarge the contribution of atomic energy to peace, health and prosperity throughout the world".

SAFETY REPORTS SERIES No. 89

DIFFUSE SEISMICITY IN SEISMIC HAZARD ASSESSMENT FOR SITE EVALUATION OF NUCLEAR INSTALLATIONS

INTERNATIONAL ATOMIC ENERGY AGENCY
VIENNA, 2016

Marketing and Sales Unit, Publishing Section
International Atomic Energy Agency
Vienna International Centre
PO Box 100
1400 Vienna, Austria
fax: +43 1 2600 29302
tel.: +43 1 2600 22417
email: sales.publications@iaea.org
http://www.iaea.org/books

Printed by the IAEA in Austria
June 2016
STI/PUB/1727

IAEA Library Cataloguing in Publication Data

Names: International Atomic Energy Agency.
Title: Diffuse seismicity in seismic hazard assessment for site evaluation of nuclear installations / International Atomic Energy Agency.
Description: Vienna : International Atomic Energy Agency, 2016. | Series: Safety reports series, ISSN 1020–6450 ; no. 89 | Includes bibliographical references.
Identifiers: IAEAL 16-01042 | ISBN 978–92–0–101716–1 (paperback : alk. paper)
Subjects: LCSH: Earthquake hazard analysis. | Nuclear facilities — Location. | Risk assessment. | Earthquake resistant design.
Classification: UDC 621.039.58: 550.348.098.7 | STI/PUB/1727

FOREWORD

One of the statutory functions of the IAEA is to establish or adopt standards of safety for the protection of health and life and the minimization of damage to property in the development and application of nuclear energy for peaceful purposes. The IAEA is also required to provide for the application of these standards to its own operations as well as to operations to which it provides assistance and, at the request of the parties to any bilateral or multilateral arrangement, to operations carried out under that arrangement, or, at the request of a State, to any of that State's activities in the field of nuclear energy.

Requirements pertaining to the seismic hazard assessment of a site and the seismic design of a nuclear installation are established, and recommendations on how to meet them are provided in IAEA safety standards. This report provides assistance on how to approach seismic hazard assessment in diffuse seismicity zones and provides further guidance on good practices in relation to the role of diffuse seismicity on seismic hazard assessment in site evaluation, to support the implementation of the relevant safety standards.

The treatment of diffuse seismicity in site evaluation differs from the practices applicable to identified seismic sources (e.g. capable faults). This report addresses the issues of the seismotectonic setting of the site and the selection of methodologies.

Regarding the seismotectonic setting of the site, diffuse seismicity is present in many different tectonic environments. It is not practical to present a unified methodology for assessing seismic hazards due to diffuse seismicity in this report. Available methodologies that accommodate varying tectonic conditions are introduced and discussed with practical examples.

Methodology selection may depend on the quality and quantity of the information available for seismic hazard evaluation. The quality and quantity may vary a great deal depending on the tectonic environment and the location of the site. In general, the amount of available geological and tectonic information in low seismicity regions is limited. Different types of methodologies to evaluate seismic hazards are introduced with their advantages and disadvantages. Embarking countries can select a methodology that is most consistent with the available quality and quantity of data.

The content of this report was reviewed at several IAEA consultants meetings, the first of which was held from in November 2012, and finalized in accordance with the recommendations of these meetings. The IAEA officer responsible for this publication was Y. Fukushima of the Department of Nuclear Safety and Security.

EDITORIAL NOTE

CONTENTS

1. INTRODUCTION

1.1. BACKGROUND

In IAEA Safety Standards Series SSG-9, Seismic Hazards in Site Evaluation for Nuclear Installations [1], earthquakes are classified into two groups: earthquakes occurring on identified seismotectonic structures, and earthquakes occurring in locations where no apparent correlation can be made with any specific geological structure. The earthquakes in the latter case are referred to as diffuse seismicity. This report describes procedures that can be used to estimate the seismic hazard in diffuse seismicity regions.

Nuclear installations have to be able to withstand earthquakes even if they are located in regions of low or diffuse seismicity. The possibility of earthquakes occurring near the site cannot be excluded and the effect has to be assessed in an appropriate way. Even earthquakes of moderate magnitude can generate ground motions of sufficient amplitude to affect the structures, systems and components of nuclear installations. Hence, in seismic hazard assessment (SHA) for nuclear installations, it is important to consider the potential contribution from earthquakes located in diffuse seismicity zones as well as the contribution from earthquakes occurring on identified seismotectonic structures.

1.2. OBJECTIVE

The main purpose of this report is to provide guidance for addressing the seismic hazard from diffuse seismicity zones to nuclear installations in a manner consistent with internationally recognized practices. This report may be used as a reference by regulatory organizations and by organizations responsible for the evaluation of seismic safety hazards for nuclear installations.

1.3. SCOPE

The scope of this report covers the treatment of diffuse seismicity zones in seismic hazard evaluations of nuclear installations. State of the art seismic hazard evaluations of diffuse seismicity relating to three issues are introduced in this publication.

(1) The seismotectonic setting may vary from site to site. Diffuse seismicity can occur in tectonically stable crustal regions, tectonically active

intra-plate crustal regions, inter-plate crustal regions, subduction regions and intra-slab regions.

(2) The quality and quantity of information available for seismic hazard evaluation varies from site to site, and may influence the approaches used to model diffuse seismicity.

(3) The method used to model diffuse seismicity should be appropriate for the specific conditions that exist at the site.

Guidance provided in this report, describing good practices, represents expert opinion but does not constitute recommendations made on the basis of a consensus of Member States.

1.4. STRUCTURE

Section 2 of this report defines a region of diffuse seismicity, considering factors such as the seismicity rate, geological information, earthquake distribution and seismotectonic setting. Section 3 presents methodologies used for the evaluation of seismic hazard in diffuse seismicity regions. Section 4 provides practical examples from different seismogenic settings and approaches used to model diffuse seismicity. A more detailed example is provided in the Appendix.

Section 5 describes methods for testing probabilistic seismic hazard analysis (PSHA) results. Section 6 describes the conclusions of this report and proposes tasks for future work.

The Appendix also discusses a project that evaluates seismic hazard in diffuse seismicity regions as a case study. The Annex contains examples of available data.

2. CHARACTERIZATION OF DIFFUSE SEISMICITY

2.1. CHARACTERIZATION OF DIFFUSE SEISMICITY

In SSG-9 [1], seismicity is classified into two categories: earthquakes occurring on identified seismotectonic structures, and earthquakes occurring on structures that are not identifiable using the current understanding of the tectonic environment in the region. SSG-9 [1] specifically states that:

"any seismotectonic model should consist, to a greater or lesser extent, of two types of seismic sources:

(1) Those seismogenic structures that can be identified using the available database;

(2) Diffuse seismicity (consisting usually, but not always, of small to moderate earthquakes) that is not attributable to specific structures identified by using the available database."

Following these definitions, this report defines diffuse seismicity zones as zones where the occurrence of earthquakes cannot be correlated with any identified seismogenic structures. Such zones are defined not only by physical phenomena but also by a functional concept derived from the lack of adequate seismic studies and databases. The potential locations of earthquakes in diffuse seismicity zones are distributed throughout the zone. Consequently, the concept of diffuse seismicity implies that if a nuclear installation site lies within a zone of diffuse seismicity, then below a certain magnitude threshold, earthquakes can occur randomly throughout the zone and can therefore potentially occur close to the nuclear installation site.

Diffuse seismicity zones are, therefore, very significant for modelling seismic hazards in regions of low and moderate seismicity where there are few identified seismogenic structures. However, diffuse seismic zones also play an important role in regions of high seismicity where diffuse seismicity is most conveniently modelled using distributed earthquake source zones rather than identified faults or seismogenic structures. Earthquakes occurring within subducting slabs are an example of this kind of seismicity, because they tend to be distributed within the slab in a relatively uniform way.

Distributed seismicity is usually modelled using the Gutenberg-Richter (GR) relation, which implies the existence of a self-similar fractal distribution of fault and earthquake sizes. However, the seismicity of large, shallow crustal-scale faults, especially strike-slip faults that form plate boundaries, is often modelled using the characteristic earthquake recurrence model [2] (in which large earthquakes on the fault may be much more frequent than the rate projected from smaller earthquakes on the fault) or the maximum earthquake model [3] (in which the maximum earthquake is considered to be the only earthquake magnitude that occurs on the fault). Especially in the maximum earthquake model, but also in the characteristic earthquake model, the smaller earthquakes may be thought of as being a separate source of seismicity that is localized on or near the fault. If the seismicity is occurring on off-fault structures in a wider zone around a fault, it may be appropriate to model it using a distributed source zone. However, if the seismicity is localized on or near the fault, it may be more effectively modelled using a seismogenic structure (fault rupture) model [4] than a distributed source zone.

2.2. SEISMICITY

Seismicity is the spatial and temporal distribution of earthquakes. From a temporal point of view, two main categories of earthquake activity rates are distinguished: low and moderate seismicity areas, and active seismicity areas.

2.2.1. Low and moderate seismicity areas

The instrumental record of seismicity is only about one century long, and historical seismicity records are often not much longer than that in many regions, and extend four thousand years at the most. Although palaeoseismology may extend the earthquake record further back in time, it is often difficult to identify seismogenic structures in regions of low or moderate seismicity, and therefore to identify where earthquakes might occur within them. It is also difficult to identify the magnitudes of the largest earthquakes that can occur, because they may not have occurred in historical time and may not have been identified in geological records based on present seismic studies and databases.

2.2.2. High seismicity areas

In seismically active regions, it is usually possible to identify seismogenic structures that are the sources of large earthquakes, as mentioned in Section 2.1. Such source zones are not discussed in this report. However, even in these regions, sources of diffuse seismicity can contribute significantly to the seismic hazard if there are not any major active source regions in the vicinity of the target site. This is especially true, if scenario based (previously termed 'deterministic') SHA is used, because that approach does not consider the rate of seismic activity. In a scenario based SHA, local earthquakes may not contribute significantly to the seismic hazard. However, in a probabilistic SHA, because of their very high frequency of occurrence, they may dominate the hazard.

2.3. SEISMOTECTONIC SETTING

Figure 1 shows epicenters of earthquakes with magnitudes larger than 4. The red dots show the distribution of earthquakes that occur in shallow crust, and the light blue or blue dots show those that occurred in deep intra-slab Wadati-Benioff zones. The locations where large earthquakes occur are concentrated in discrete regions, and most of them occur on identified seismic structures. However, a significant portion of earthquakes occur as diffuse seismicity.

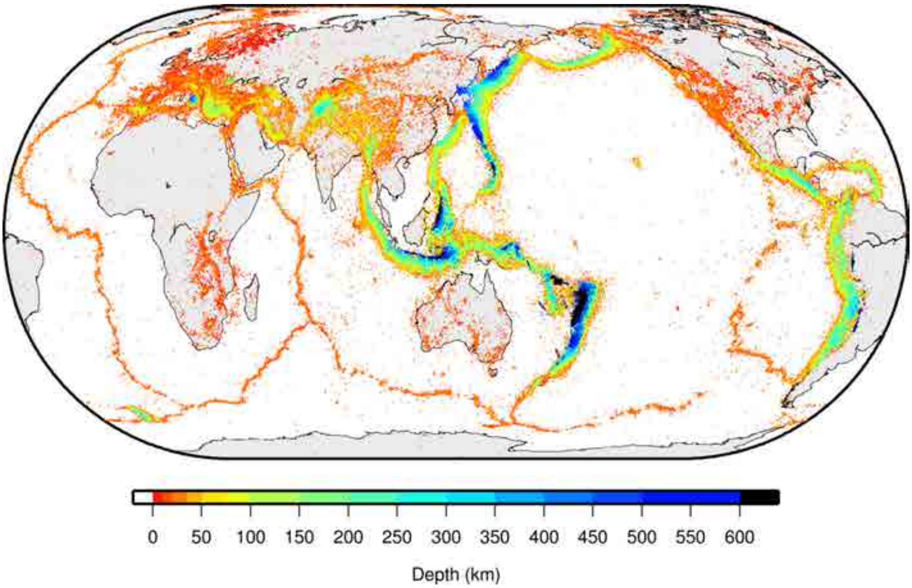

FIG. 1. Worldwide earthquake source distribution 1960–2013 with magnitude larger than 4 (reproduced from the International Seismological Centre (ISC) web site with permission).

Diffuse seismicity occurs in different seismotectonic settings and involves various different types of earthquakes. First, the seismotectonic setting of the site region needs to be identified. This can be done by analysing the overall tectonic environment. The following sections describe several tectonic environments and describe how diffuse seismicity may occur within these tectonic environments.

Figure 2 is a schematic diagram of a subduction plate boundary and the types of large identified earthquakes that occur within it [5]. Figure 3 is a schematic diagram of two types of crustal plate boundaries showing a transform fault zone and a crustal collision zone (not labelled). Away from plate boundaries like those shown in these two figures, seismicity is generally low, reflecting the tectonic stability in regions that are remote from the plate boundaries. Diffuse seismicity usually, but not always, consists of small to moderate earthquakes that are not attributable to specific structures identified by using the available database. In particular, the concept of diffuse seismicity implies that, at least below some magnitude threshold, earthquakes can occur randomly throughout a region and can therefore potentially occur close to a nuclear installation site. Diffuse seismicity can occur in each of the following tectonic environments. The first two are end members of a continuum of tectonic environments.

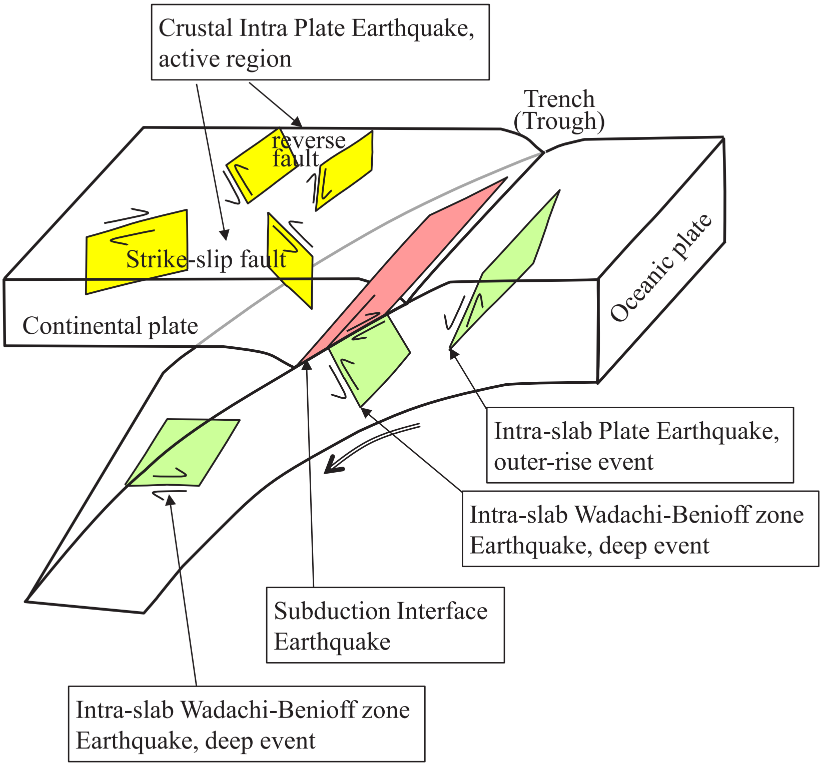

FIG. 2. Schematic diagram of types of large earthquakes occurring in a subduction zone (reproduced from Headquarters for Earthquake Research Promotion (HERP) [5] with permission).

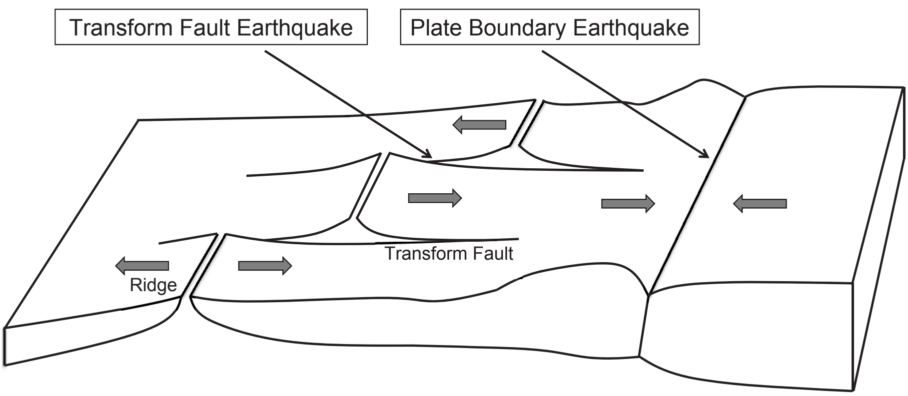

FIG. 3. Schematic diagram of large crustal plate boundary earthquakes in transform zones with strike-slip faulting and rifts with normal faulting (left) and in a plate collision zone with reverse faulting (right).

These figures are not only relevant to diffuse seismicity but also to the seismicity of identified earthquake sources, as well as being helpful in the identification of sources.

2.3.1. Crustal intra-plate earthquakes in tectonically stable continental regions

Earthquakes that occur in the continental crust away from plate margins are described as crustal intra-plate earthquakes in tectonically stable continental regions. They are relatively infrequent, but their magnitudes can be quite large. Identified seismic sources are usually not well determined in this type of tectonic setting, and diffuse seismicity generally dominates the seismic hazard. It is important to evaluate the regional characteristics of the seismicity and tectonics in these zones. Information from palaeoseismology may provide valuable data for estimating the magnitudes of the largest possible earthquakes in these regions.

2.3.2. Crustal intra-plate earthquakes in tectonically active plate boundary regions

In crustal intra-plate regions close to active plate margins, such as the Japanese archipelago, there are regions where seismicity is very high. Most large earthquakes along active plate boundary regions occur on active fault systems and are associated with identified faults. However, as mentioned in Section 2.1, diffuse seismicity may also exist in the vicinity of these active regions. Earthquakes also occur on unidentified, off-fault structures in a wider zone around the faults. In this case, it may be appropriate to model such seismic activity using a distributed seismicity source zone. However, if the seismicity is localized on or near an identified fault, it may be more effectively treated using a seismotectonic fault model.

2.3.3. Crustal plate boundary earthquakes

Examples of transform fault zones like the one shown on the left of Fig. 3 include the San Andreas Fault system in California and the Anatolian fault system in Turkey. An example of the crustal collision zone (not labelled) shown on the right of Fig. 3 is the collision zone between the Indian plate and the Eurasian plate. Most large earthquakes on these fault systems are associated with identified seismotectonic structures because the source faults are clearly identified on the ground surface. However, as mentioned in Section 2.1, diffuse seismicity may also be present if it is occurring on unidentified off-fault structures in a wider zone around a fault. In this case, it may be appropriate to model the diffuse seismicity using a distributed source zone. However, as for the case of intra-plate earthquakes, if the seismicity is localized on or near the identified fault, it may be more effectively treated using a seismotectonic structure model rather than a distributed source zone.

2.3.4. Subduction interface earthquakes

Most large subduction earthquakes occur offshore, relatively distant from land. In this situation, the contribution of diffuse seismicity, if present in the plate interface region, is expected to be negligible. However, in locations where the shallow plate interface is close to shore, such as beneath Tokyo, Japan, and Wellington, New Zealand, the potential contribution of diffuse seismicity may require consideration.

2.3.5. Intra-slab Wadati-Benioff zone earthquakes

Intra-slab earthquakes occur within the subducting oceanic plate in the Wadati-Benioff zone, generally at depths greater than 30 km, and are shown in Fig. 1. Since it is difficult to identify the faults on which these earthquakes occur, it is most convenient to treat them as diffuse seismicity occurring within distributed seismic source zones. The depth and magnitude distributions of the events, which are required for SHA, may be based on records of historical seismicity. To identify the depth ranges of diffuse seismicity, the Wadati-Benioff zone in the target area should be evaluated.

2.3.6. Intra-slab outer rise earthquakes

Intra-slab earthquakes also occur oceanward of the trench at shallow depths within the oceanic plate, as shown in Fig. 2. The locations and magnitudes of this category of earthquakes are difficult to estimate, and detecting potential source faults may require expansive and detailed marine geophysical surveys. Hence, it is most convenient to treat these regions as diffuse seismicity regions in SHAs. The depth and magnitude distribution of the events, knowledge of which is required for SHA, may be based on records of historical seismicity. Diffuse seismicity in the outer rise does not usually dominate ground motions at nuclear installations, because these types of earthquakes occur far offshore. However, the potential impact and contribution to the total hazard should be considered in probabilistic SHA.

2.4. CONSISTENCY WITH PALAEOSEISMOLOGY

Palaeoseismological approaches are powerful tools for seismic source characterization efforts in diffuse seismicity regions [6]. In the absence of long term direct measurements of earthquake activity and identifiable seismogenic fault structures in diffuse seismicity zones, palaeoseismological investigations may provide critical information to identify past large earthquakes and their occurrence rates in such regions.

From a seismological perspective, surface faulting is the result of coseismic crustal faulting that reaches or at least deforms the ground surface. They are the most common causes of strong ground motion. Magnitude is related to seismic moment and is therefore dependent on the size of the rupture (area) and the amount of displacement. Therefore, the measurement of minimum slip in palaeoseismological trenches and the length of the surface fault rupture represent essential parameters for magnitude estimate, also via empirical relationships. However, the boundary between buried and surface-breaking earthquake magnitudes is area dependent.

If enough data is gathered, the curve shown in Fig. 4 can shift towards the lower magnitudes. If a regional seismotectonic source is considered as uniform, it must be accepeted that unidentified earthquakes of larger magnitudes may have occurred; consequently, the curve can shift towards the higher magnitudes. Seismic hazard studies may need to take into account such uncertainties. This is essential in areas of especially high seismicity. For example, the 2000 earthquake in West Tottori, Japan (M_J 7.3, M_W 6.6), occurred without an identified capable

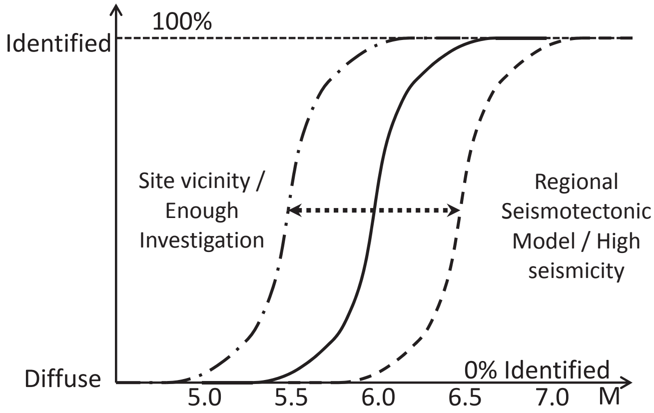

FIG. 4. A simplified overview of the identification rate of seismic sources. The rate of identification of seismic sources increases gradually with earthquake magnitude. Diffuse seismicity has an identification rate of zero. Please note that the values shown are not precise.

fault. Based on the data in active areas, Shimazaki [7] suggested in 1986 that the border of surface-breaking shallow seismicity is a moment magnitude (M_W) of 6.5 (M_0 = 7.5 × 10^{18} N·m). This magnitude level might be an average recommendable for active regions.

However, if detailed and careful geological, geomorphological, geophysical and seismological investigations are conducted at the target site, the level of required magnitude can be decreased according to expert judgements and data. SSG-9 [1], in section 3, paras 3.3 and 3.4, provides guidance on the conduct of investigations:

> "Investigations should be conducted on four spatial scales — regional, near regional, site vicinity and site area — leading to progressively more detailed investigations, data and information...seismogenic structures in the near region and in the site vicinity will usually be more important for seismic hazard evaluation".

From the point of view of seismic safety, maximum magnitudes in excess of 6 are possible in zones of diffuse seismicity, but magnitudes may not be too much larger than this value. If magnitudes exceed this value, the causative faults will likely be identified and would appear in the geomorphological, geological and/or geophysical databases. In high seismicity regions, however, the maximum magnitude can be increased. With expert judgement and a consideration of the uncertainties, it can be determined whether the maximum magnitude is suitable for ground motion evaluation. Palaeoseismological approaches can provide critical data to be used in expert judgement. It should be also taken into account, however, that particularly at crustal intra-plate compressive settings, morphogenic earthquakes may have a threshold magnitude of around 7 and causative faults are usually elusive, because of the lack of diagnostic morphologies and relationships with seismicity.

3. METHODOLOGY OF SEISMIC HAZARD ASSESSMENT IN REGIONS OF DIFFUSE SEISMICITY

3.1. INTRODUCTION

The final goal of a SHA is to evaluate the seismic hazard at the site of interest. This seismic hazard is, in most cases, expressed in terms of a certain measure of the ground motion, which is usually acceleration, but could also be velocity or displacement. If the methodology is probabilistic, the ground motions will be obtained for different probabilities of exceedance, a result which is usually described in terms of a seismic hazard curve. If the methodology is so-called scenario based SHA, the result will simply be a point estimate of the selected measure of the ground motion.

In regions of diffuse seismicity, model parameters required to perform seismic hazard evaluations are the same as those in regions with identified sources. However, a difficulty in regions of diffuse seismicity is the scarcity of data to constrain seismic source model parameters. These regions often lack the type and amount of data needed to develop adequate model parameters. This section is intended to provide guidance on how to assess and quantify the necessary seismic source model parameters for regions with diffuse seismicity.

The various tasks performed in a SHA can be subdivided into subtasks as listed in Section 3.8.

3.2. EARTHQUAKE CATALOGUE

Diffuse seismicity is generally modelled using PSHA, in which an earthquake catalogue plays a very important role, since it constitutes the primary, if not the sole source of information for characterizing rates of seismic activity. The information contained in the earthquake catalogue can come from instrumental records, historical records and from palaeoseismology. Whatever the origin of the information, all earthquakes in the catalogue need to be described with a uniform magnitude measure (such as M_W). Seismic activity rates should be based on this magnitude type and the uniform magnitude scale should be consistent with those used by the GMPE (see Section 3.2.2).

3.2.1. Earthquake catalogue compilation

It may be necessary to combine several earthquake catalogues, which may often be catalogues provided by different institutions, to make a uniform catalogue for the target area. Some international institutions provide earthquake catalogues that can be employed either as a starting point or, if the area of interest is not covered by any other national institution, as the only source of information. Some examples of international catalogues follow.

The ISC compiles the ISC Bulletin, which relies on data contributed by over 130 seismological agencies from around the world and is regarded as a comprehensive record of the Earth’s seismicity. It contains data from 1904 to the present, although its review processes mean that it is typically 24 months behind the current date. For each earthquake, the bulletin provides the information available from all the agencies that have contributed information for that event.

The Global Earthquake Model Foundation, in collaboration with the ISC, has developed two earthquake catalogues covering the historical and instrumental periods, respectively. The Global Historical Earthquake Catalogue, developed by an international consortium, spans from 1000 to 1903 and contains around 1000 earthquakes with estimated magnitudes above M_W 7.0. Taking an average rate of worldwide earthquakes with M_W greater or equal to 7.0 of between 15 and 20 events per year, the number of earthquakes included in this historical catalogue is around 7% of the estimated actual earthquakes. The instrumental catalogue was developed by a team of international experts led by the ISC, and covers some 110 years, starting in 1900. Among its most relevant characteristics is that it is homogeneous in location and magnitude M_W estimates.

These two catalogues have a common origin to a large extent; however, the way in which the information is provided differs in each case: the Global Earthquake Model catalogue is expected to be employed in SHA, and hence the information it includes and the way this is provided is orientated to that purpose. By contrast, the ISC catalogue provides all the available information for each event from many institutions; it is more relevant for seismological research but it may be useful in an SHA when specific insight on some events is needed.

Another example that covers the European area is the Seismic Hazard Harmonization in Europe (SHARE) catalogue. The SHARE European Earthquake Catalogue, compiled in the frame of Task 3.1 of the SHARE European Project, consists of two portions:

— The SHARE European Earthquake Catalogue (SHEEC) 1000–1899, compiled under the coordination of the Italian Istituto Nazionale di Geofisica e Vulcanologia, builds on the data contained in the Archive of Historical Earthquake Data (AHEAD) [8].
— The SHARE European Earthquake Catalogue (SHEEC) 1900–2006 compiled by the GFZ German Research Centre for Geosciences. This part of the catalogue represents a temporal and spatial excerpt of the European-Mediterranean Earthquake Catalogue for the last millennium [9] with some modifications, which are described in Ref. [10].

The United States Geological Survey provides information on earthquakes worldwide immediately after they happen. It maintains the Advanced National Seismic System (ANSS) Comprehensive Catalog. This also consists of the Preliminary Determination of Epicenters Bulletin, the Shake Map Atlas and the Centennial Earthquake Catalog.

Two issues have to be considered when combining earthquake catalogues:

(1) Magnitude/intensity scales can be different in different catalogues.
(2) The regions covered by different catalogues may overlap, requiring a careful selection process to avoid duplication.

Guidance and recommendations for the first point will be given in Section 3.2.2. Concerning the second point, careful editing is required to avoid the duplication of earthquakes if more than one record for the same event exists in different catalogues. Different catalogues may provide different locations and magnitudes for the same event. In such cases, the more authoritative catalogue should be identified and the best justified location and magnitude should be used in the merged catalogue.

Algorithm programming for automating the task of combining instrumental catalogues may be feasible, but this is very complicated when dealing with historical events that usually have large epicentral or intensity uncertainties. In this case, the merging will most likely be done manually with the help of graphical representations. Even in the case of instrumental catalogues, a sample manual check should be performed, at least for larger earthquakes.

3.2.2. Uniform magnitude

Regional instrumental catalogues often use local magnitude scales. For example, the Japan Meteorological Agency (JMA) uses the Japan Meteorological Agency seismic intensity scale (M_J). Other countries use magnitude scales such as the Richter magnitude scale (M_L), the surface wave magnitude (M_s), the body wave magnitude (m_b or m_B) and Lg wave magnitude (m_{Lg}). However, all these scales experience saturation above different levels of magnitude. In general, such magnitudes present both advantages and disadvantages depending on the region and/or the size of the earthquake.

The most recent and most commonly used earthquake magnitude scale is the moment magnitude (M_W) which is derived from the seismic moment (M_0) of an earthquake using the following relationship (see Refs [11, 12]):

$$M_W = \frac{2}{3}\left(\log M_0 - 9.1\right) \tag{1}$$

where M_0 is seismic moment in N·m.

$$M_0 = \mu S D \tag{2}$$

Seismic moment is defined as a product of the rupture area (S), dislocation (D) and rigidity (μ), in N·m, at the point where the earthquake occurs. Consequently, moment magnitude reflects the physical behaviour of fault rupture and does not saturate, unlike other magnitude scales that are mostly based on observed amplitudes of seismograms.

As indicated above, a uniform magnitude scale should be used in the earthquake catalogue. Moment magnitude, M_W, is generally used for this purpose. It is also the preferred magnitude scale in most recently developed GMPEs.

Figure 5 shows the difference between several magnitude scales and the moment magnitude [13]. This plot also shows the saturation problem mentioned above for magnitude scales other than the moment magnitude. For transforming local magnitudes into moment magnitudes, various relationships are employed depending on the type of magnitude scale being converted and the region in which it is used. The regional dependence is particularly evident in the case of the Richter magnitude scale, M_L, which depends on the detailed procedures applied by the institution estimating the local magnitude. M_L may differ significantly among countries and/or institutions; hence, conversion from M_L to M_W should be performed carefully.

Earthquakes from historical records will often be quantified in terms of maximum intensity, although for large earthquakes it is very likely that specific studies estimating their magnitudes exist. As in the case of magnitude scales, there are also several different intensity scales employed around the world.

Once the different types of magnitudes or intensities in the earthquake catalogue have been identified, appropriate relationships need to be developed or selected to convert other magnitude scales to the uniform magnitude scale of choice (usually M_W). The relationships should be well justified and widely accepted for the area of interest. They should also provide a quantification of the uncertainty, so as to allow for the calculation of the total uncertainty associated with the final magnitudes, which will be a composition of the uncertainty associated with the original magnitude measure and uncertainties introduced during the conversion process.

3.2.3. Declustering catalogue

In most PSHAs, a Poissonian assumption is made at some point in the calculation. This assumption relies on the fact that the earthquakes used for calculating seismic activity rates are independent of one another. Identifying independent earthquakes from other earthquakes listed in the catalogue developed for the region requires a process called declustering.

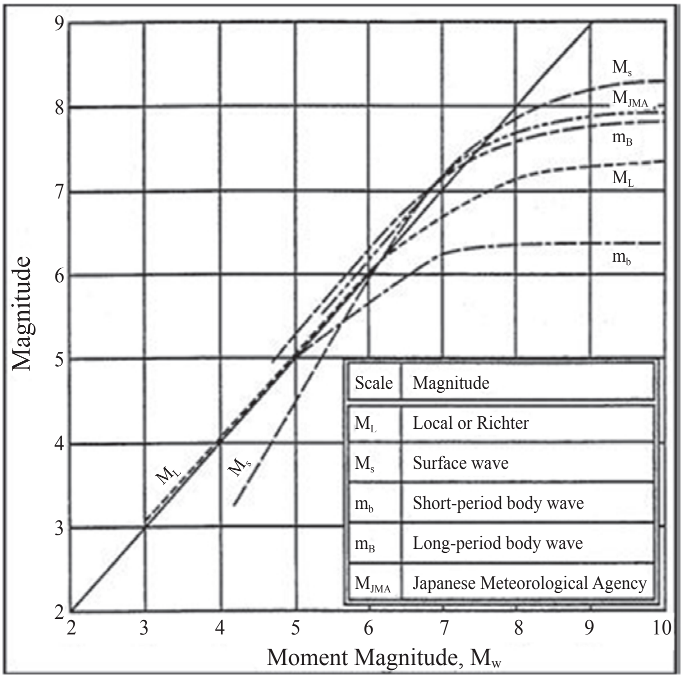

FIG. 5. Comparison of Earthquake Magnitude Scales (figure courtesy of Springer [13]).

Because earthquakes usually occur in clusters, they can be classified into three main groups:

— Main shock: the largest earthquake. It is usually, although not always, significantly larger than the rest in the series.
— Foreshocks: earthquakes occurring before the main shock, and close to it in time and space.
— Aftershocks: earthquakes occurring after the main shock, and close to it in time and space.

There is always a certain degree of subjectivity when cataloguing an event as a foreshock or aftershock. While aftershock activity is quite common following a main shock, this is not the case for foreshock activity. Foreshocks usually span a shorter period of time than aftershocks, and there are many cases of large earthquakes for which no foreshock activity was observed.

The two most widely employed methodologies for identifying foreshocks and aftershocks with the purpose of eliminating them from the earthquake catalogue are those proposed by Gardner and Knopoff in 1974 [14] and by Reasenberg in 1985 [15].

The Gardner and Knopoff [14] methodology consists in centering a time and space window on the main shock, and considering all the events located inside both windows foreshocks or aftershocks. The window sizes depend on the main event's magnitude. Gardner and Knopoff proposed a specific dependence adjusted for the seismicity in California. Their values could be considered reference values, but appropriate values adapted to the local seismicity should be employed.

Reasenberg's algorithm [15] allows the linking of aftershock triggering within an earthquake cluster. Identified aftershocks can have their own aftershocks, and all identified events are considered to belong to one common cluster. Only the largest earthquake is finally defined as the cluster's main shock. Another important characteristic of this method is that the space–time distance is based on Omori's law, which states that the rate of aftershocks depends on the time that has passed since the main shock.

3.2.4. Catalogue completeness

As indicated in Section 3.1, the information contained in an earthquake catalogue can come from instrumental records, from historical records and from palaeoseismology. Because the earthquake catalogue can never be complete for all magnitude ranges, and because the time period of interest potentially goes back hundreds of years, if not thousands, it becomes a critical issue to characterize the completeness of the earthquake catalogue prior to calculating rates of earthquake activity in regions of interest. In the instrumental or historical catalogues, completeness will vary depending on the magnitudes of earthquakes (in an historical catalogue, large magnitude earthquakes are more likely to be registered than smaller ones) and/or their locations (whether they have a land or marine epicentre and occur in populated or unpopulated areas). The information on completeness is a key parameter when calculating the seismic activity rate, as described in Section 3.3.

When determining the catalogue's completeness, the objective is to establish the year after which the catalogue can be considered complete for a given magnitude. Usually a completeness year is calculated for predefined magnitude intervals. As expected, as the magnitude increases, the period of completeness becomes longer.

Methodologies for establishing completeness years can be subdivided into two types:

- — Graphical methodologies, which are the simplest and most intuitive;
- — Mathematical methodologies, which require some kind of programming or the use of an already available algorithm.

Graphical methodologies consist of visual inspections of one or more representations of occurrence of earthquakes against time. The simplest representation consists of plotting magnitudes against time [16]. For each magnitude interval, the cumulative number of earthquakes is plotted against time, and a change in the curvature is observed around the year of completeness. The identification of completeness years involves a certain degree of subjectivity.

Mathematical methodologies (such as those of Albarello et al. [17]), on the other hand, rely on the assumption of the stationarity of seismic processes. This approach requires a declustered earthquake catalogue. To consider the approach, the mean, variance or any other statistical moments should be stationary. The point at which the stationarity is lost indicates the completeness point. The best known methodology is that proposed by Stepp in 1971 and 1972 [18, 19].

Both methodologies can also be combined in a single hazard assessment. Mathematical methodologies usually work better for low magnitude intervals than for large magnitudes, for which they tend to produce very short completeness periods. Another common assumption made in this respect is that if the catalogue is considered to be complete for a certain range of magnitudes, it is also complete for higher magnitudes. A graphical methodology can then be carried out to provide results for larger magnitudes and to also be a verification of the results obtained with the mathematical approach for the lower magnitudes.

Not only temporal completeness, but also spatial completeness should be verified by plotting the earthquake epicentres on a map. Following these procedures, a single coherent earthquake catalogue with a uniform magnitude scale, including its completeness records, is compiled in the target area.

3.3. SEISMIC ACTIVITY PARAMETERIZATION

The parameterization of diffuse seismicity is discussed in paragraphs 4.31 and 4.32 of SSG-9 [1]. The traditional procedure for characterizing diffuse seismic activity has been to use available seismic, geological and tectonic information to construct a series of non-overlapping seismic source zones. Each of these zones is assumed to have uniform seismicity. The discrete character of the information in the earthquake catalogue is smoothed by uniformly distributing over each zone the seismic activity manifested by the earthquakes that occurred in that zone in the past. Recorded seismic activity varies with location, but it is assumed to be uniform over each zone. SSG-9 [1] also states in paragraph 4.28 that non-uniform distributions of seismicity can also be used, if supported by available data. Consequently, the methodologies that forego the use of individual seismotectonic zones are also acceptable.

3.3.1. Traditional zoned approach

The first task is to establish the geometry of the seismic source zones to be used. Source zones should be identified for the region where, if they occurred, earthquakes would influence the seismic hazard at the site of interest. A commonly used reference distance for identifying seismic sources is typically 300 km, as indicated in SSG-9 [1]. Sources capable of producing very large magnitude earthquakes that could impact the hazard at even greater distances should also be identified. In most cases, however, the seismic activity representing such large earthquakes will be modelled directly with explicit faults. In regions where higher seismicity rates are observed outside the reference distance, a sensitivity study may need to be conducted to determine whether such seismic sources contribute to the seismic hazard. In stable tectonic regions, the attenuation of ground motion with distance is usually more gradual than in tectonically active regions. Hence, in such tectonic regions, a larger reference distance may be required.

The characterization of seismic source zones can be a difficult task and it is often the subject of controversy. It involves multidisciplinary considerations, taking into account all the available seismic, geological and tectonic information. When published zonation models that have already been subjected to expert reviews or widely accepted by the scientific community are available, it might be a good option to adopt such zonation directly or to use the models as a starting point for the development of a new zonation.

As pointed out at the beginning of Section 3.3, the traditional methodology is to use uniform activity rates in each zone. The seismic source zones to be defined are expected to incorporate the seismic activity occurring along unidentified faults. In this concept, the seismic source zones are usually constructed by trying to find a spatial correlation between earthquake epicentres and large scale geotectonic units. This procedure may suffer from subjectivity, resulting in zones of different shapes and sizes depending on the analysts that perform the study. In areas of low or medium seismicity, the task may become especially complicated.

Most crustal seismicity occurs in the upper crust. Hence, it is the one of the critical zones to be studied. The original motivation was the apparent correlation between the occurrence of earthquakes and geological structure [20]. The detailed study of these geological parameters around the studied area can introduce some objectivity in the definition of the zones.

With regard to seismicity, it is important to determine not only epicentres, but also focal depths within the upper crust, and to evaluate the number of events per unit volume rather than per unit area.

The seismogenic zones can be defined as regions exhibiting similar characteristics in both geological and seismicity parameters. Once the geometries of the seismic source zones have been established, each zone has to be assigned seismic activity parameters. These could be constant over each zone, or they could vary. The two models that are used more frequently to describe the recurrence of earthquakes in seismic sources are the GR relation [21] and Schwartz and Coppersmith's characteristic earthquake model [2]. The latter focuses on identified faults with a known recurrence period; therefore it is not considered particularly suitable for dealing with diffuse seismicity.

In 1944, Gutenberg and Richter [22] proposed a linear relationship between the number of earthquakes that occur within each magnitude range $M_i \pm \Delta M$ and the reference magnitude M_i for that range. Richter [21] modified this to employ instead the cumulative number of earthquakes with magnitudes greater than or equal to M, thus establishing the following linear relationship:

$$\log N(M) = a - bM \tag{3}$$

where $N(M)$ is the annual number of earthquakes of magnitude greater than or equal to M, M is the selected magnitude measure and a and b are the seismic parameters to be determined for each seismogenic zone.

It can be easily derived that the annual activity rate for earthquakes of greater than or equal to magnitude M can be obtained as follows:

$$N(M) = 10^{a-bM} \tag{4}$$

In most cases, a Poissonian assumption is made at some point in the SHA, which mathematically implies going through exponential operations. As a consequence, it is quite common to express the previous relationship employing the natural logarithm, which leads to the expression:

$$\ln N(M) = \alpha - \beta M \tag{5}$$

where α and β are the new parameters to be adjusted

It is easy to see that the parameters a, b, α and β are related as follows:

$$\alpha = a \ \ln \ 10 \tag{6}$$

$$\beta = b \ \ln \ 10 \tag{7}$$

Figure 6 shows the data and the least-square fit originally presented by Richter in 1958 [21] for Southern California, in which $a = 5$ and $b = 0.85$.

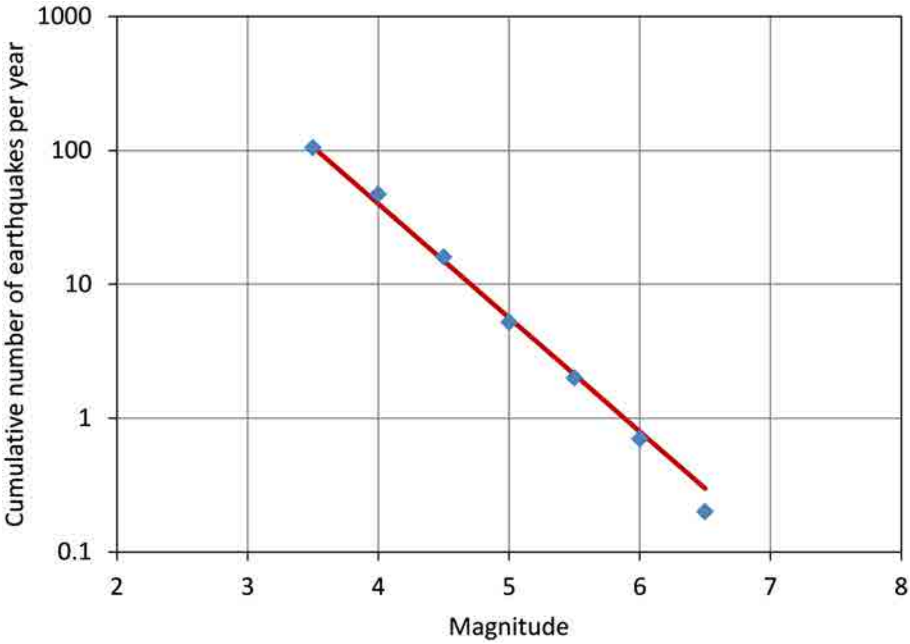

FIG. 6. Least-square fit of Southern California earthquake activity based on data from Richter [21].

In traditional SHA, the parameters have to be fitted for each seismogenic zone. The steps to follow are:

— Choosing reference magnitude levels, M_i;
— Calculating the frequency distribution of earthquakes (annual number of earthquakes for each magnitude, N_i);
— Curve-fitting the pairs (N_i, M_i) to obtain the *a*- and *b*-parameters in Eq. (3);
— Deciding on the range of applicability of the GR relationship obtained.

The methodology for fitting the data employed by Richter [21] was a simple least-square fit of Eq. (3). He also considered a single time period for all the magnitudes. However, the cumulative event counts are not independent, hence the least-square fit is questionable; also, the completeness of the catalogue may be expected to differ for different magnitude levels, an aspect that needs to be studied according to the recommendations indicated in Section 3.2.4. A number of methodologies have subsequently been proposed and adopted to address these limitations. In 1965, Aki [23] first raised the issue of the maximum likelihood methods for estimating the GR *b*-value; Molchan et al. [24] divided the number of events by the time interval of completeness for each magnitude interval as a maximum likelihood estimator. In 1980, Weichert [25] proposed a maximum likelihood estimation of the GR parameters for events grouped in magnitude intervals with each group observed over individual time periods. More recently, in 2012, Kijko and Smit [26] proposed an extension of Ref. [23] which particularly addressed the consideration of the use of multiple catalogues of different levels of completeness, which is an alternative to Weichert's solution [25].

A general recommendation is that the maximum likelihood estimator should be employed for deriving the GR parameters. At present, the maximum likelihood estimator proposed by Weichert [25] is very commonly employed. Irrespective of the methodology employed for fitting the parameters, the determination of the catalogue completeness remains a key task, as discussed in Section 3.2.4.

The GR *b*-parameter is commonly referred to as the GR *b*-value or just the *b*-value. It indicates the ratio between the numbers of large and small earthquakes. For every magnitude 6.0 event, there will be 10^{b} magnitude 5.0 events, 10^{2b} magnitude 4.0 events, and so on. GR *b*-values typically range between 0.5 and 1.5, although the range of variation is likely to be smaller within the region examined for a specific SHA. The GR *b*-value is considered to be characteristic of the tectonic environment, and hence it is common to find regional studies of the *b*-value that are useful as a reference. The distribution of the GR *b*-values in the region of interest is informative, and 2-D plots are helpful for visualizing the range of *b*-values and the variability around the site. Examples of such plots are presented in Fig. 7 for two different zonations.

The GR *a*-parameter is a measure of the rate of seismic activity and can have very different values. Hazard results usually show a higher sensitivity to the *a*-value than to the *b*-value. In general, there is no problem in assessing the GR *a*-value, no matter the size of the zones; however, for regions with low seismicity, the determination of the *b*-value can be challenging owing to the scarcity of data. In such cases, one option may be to calculate a regional *b*-value with data from several adjoining zones, or to estimate it from studies in other regions that are thought to have similar seismicity. In any case, the criteria for the delineation of zones should never be influenced by needs while deriving the GR parameters.

When dealing with diffuse seismicity, seismic activity can be adequately represented in most cases with a single pair of GR parameters (i.e. a single line).

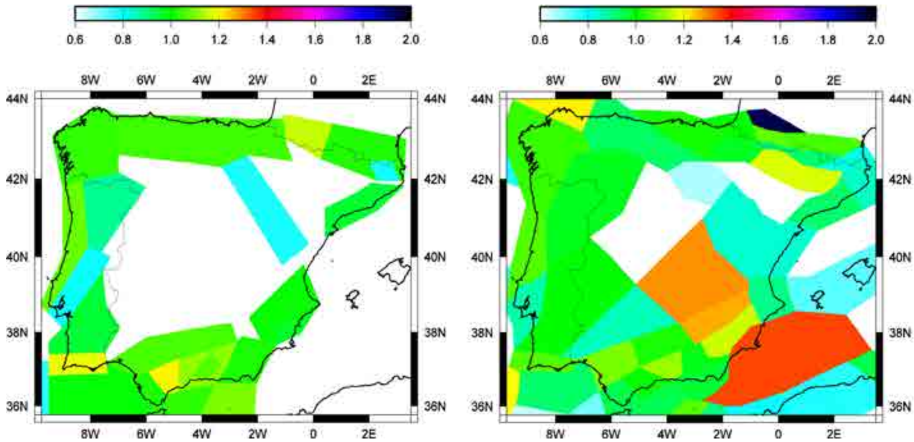

FIG. 7. Plots of the GR b-value for two zonations of the Iberian Peninsula, courtesy of M. Crespo.

When more than one tendency is observed, it is worth verifying whether the completeness of the catalogue has been duly incorporated and whether suitable magnitude measures are being used. If the deviation from a single logarithmic line is confirmed, a bilinear GR approach can be implemented, using different slopes for the lower and upper magnitude ranges.

When obtaining the value of the GR parameters, both *a* and *b*, a measure of their uncertainty should also be determined. This uncertainty should be adequately incorporated in the global SHA.

3.3.2. Zoneless approaches

In zoneless approaches, the seismic activity rate is calculated using the declustered earthquake catalogue without delineating any seismogenic zones over which the activity rate will be assumed to remain constant. The idea is to allow the expression of the seismic catalogue without biasing the shape of the activity rate function. The dependence on location has a continuous variation (as opposed to forcing it to be constant over certain zones), while the dependence on magnitude does not necessarily follow the GR relation.

These methodologies use non-parametric density estimation, in which the objective is to find the density function from which a given sample derives, without specifying a priori a specific shape for the density function, such as a normal distribution or a Gamma one; instead, the shape of the distribution is expected to be provided by the sample itself.

The most basic form of non-parametric density estimation is the histogram. The space over which the sample is distributed is divided into cells that are usually uniform in shape and size, although this is not a formal requirement. For each cell, the number of elements (seismic events in this case) is computed, with the final function acquiring a constant value over each bin that is proportional to its number of events. An example of histograms constructed with events of a magnitude between 4 and 5 around the Iberian Peninsula is presented in Fig. 8. As mentioned above, the concept of the histogram was introduced to the study of seismic activity by Frankel in 1995 [27] for computing the GR *a*-value. An improvement by Frankel with respect to the traditional formulation of the histogram with step functions was to centre a smooth function that decays with distance from the centre of the cell.

Another improvement with respect to the histogram is the naive estimation. The method relies on centering a density function on each element of the sample (instead of on each cell), adding up all such functions and then normalizing their sum. The smooth function can be any unit density function. It was initially proposed by Fix and Hodges in 1951 [28], but a more recent and very clear description was provided by Silverman in 1986 [29]. The shape of the kernel function and its spatial extent have to be decided by the user, as is the case for the width of the bins in the histogram.

The mathematical definition of the density estimated with kernel functions is as follows:

$$f_n(\boldsymbol{x}) = \frac{1}{nH^2} \sum_{i=1}^{n} K\left(\frac{\boldsymbol{x} - \boldsymbol{x_i}}{H}\right) \tag{8}$$

where

n is the number of elements in the sample

H is the bandwidth, a measure of the separation between sample elements

K is the kernel function

And $\boldsymbol{x}_i$ is the position of event i.

An example of kernel density estimation, constructed with the same events as in Fig. 8 (magnitude between 4 and 5 around the Iberian Peninsula), is presented in Fig. 9.

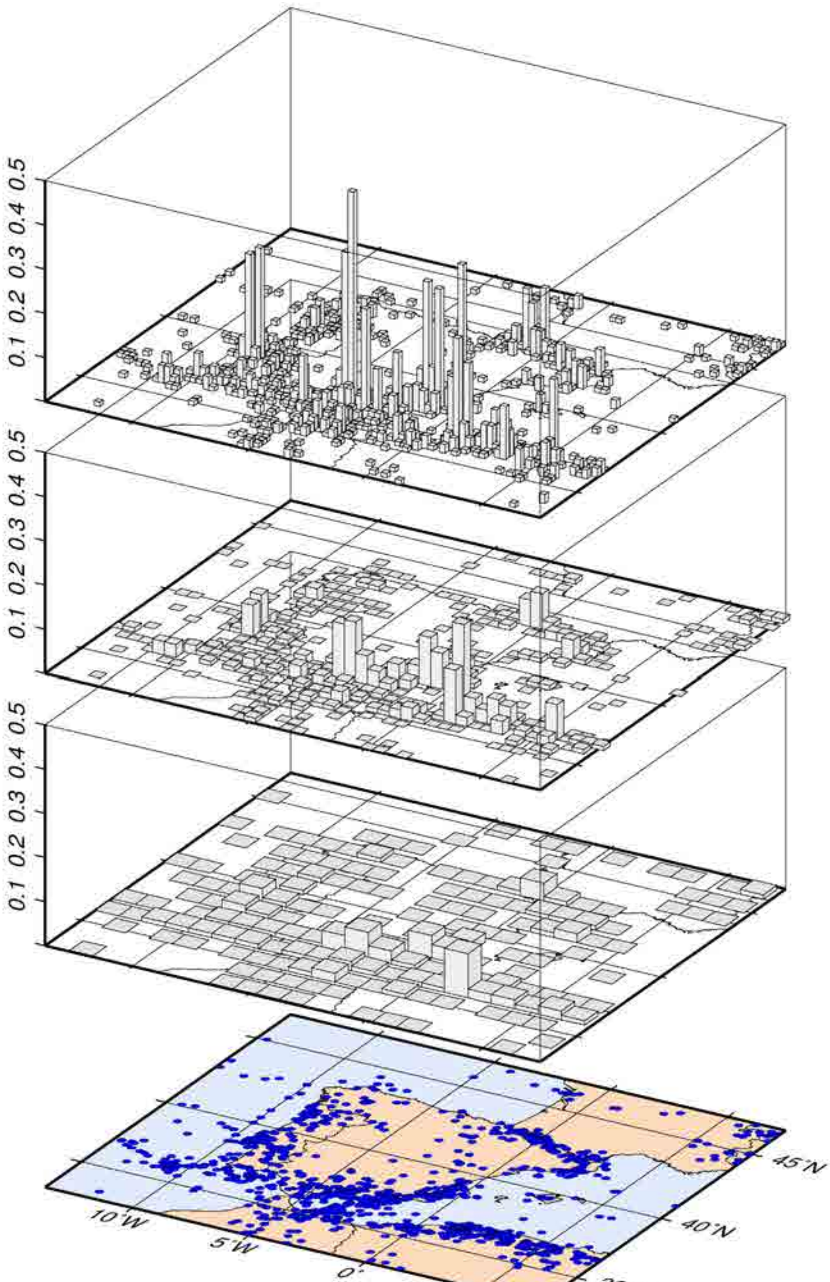

FIG. 8. Histograms for events around the Iberian Peninsula with magnitude M_W between 4.0 and 5.0. The bin sizes considered, from top to bottom, are 0.25°, 0.5° and 1° respectively. Image courtesy of M. Crespo.

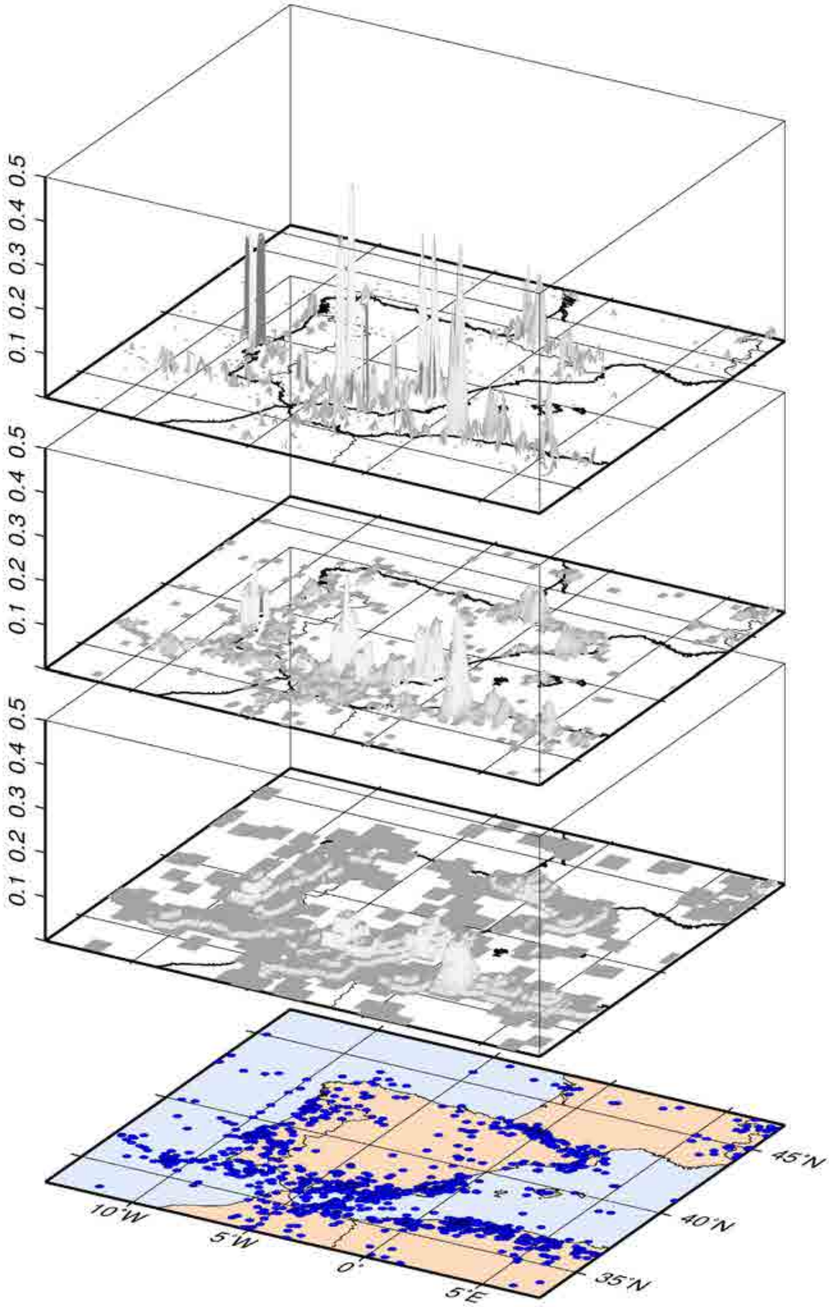

FIG. 9. Kernel estimations for events around the Iberian Peninsula with magnitude M_W between 4.0 and 5.0. The kernel bandwidths considered, from top to bottom, are 0.25° 0.5° and 1° respectively. Image courtesy of M. Crespo.

For generating a density, λ_k, of the seismic activity rate, two changes are introduced in Eq. (8):

— The normalization with respect to the number of events, n, is omitted, thus the result is expressed in terms of number of events.
— Each kernel function is divided by an effective period, T, so the density of events is expressed per unit time.

With the above two changes, the expression becomes:

$$\lambda_k(M,\boldsymbol{x}) = \frac{1}{[H]^2} \sum_{i=1}^{n} \frac{K\left(\frac{\boldsymbol{x}-\boldsymbol{x_i}}{H}\right)}{T(\boldsymbol{x_i})} \tag{9}$$

The kernel function, K, the effective detection period, T, and the bandwidth, H, are the three main parameters that influence the activity rate density.

The effective period, T, ensures that the function has the desired units of events/year, as is necessary for a seismic activity rate. Its value is such that the total number of events of the same type, divided by the effective period, yields the actual seismic activity rate. As noted in Eq. (9), each event can be assigned a different effective period, T, which makes the methodology very versatile. Typical event characteristics on which the effective period usually depends are the event magnitude, the time of occurrence and the type of epicentral location (onshore or offshore, and whether the area was populated at the time of occurrence), but other factors that affect the probability of detection can also be incorporated in the effective period.

The resulting activity rate density, λ_k, depends on location as well as magnitude through the bandwidth, H. As can be seen, it is a summation of kernel functions, K, placed on each event of the catalogue with coordinates $\boldsymbol{x}_i$. Each function is weighted with an effective detection period, T; the normalization is achieved through the bandwidth, H, which depends on the distance between events. The fact of dividing by H^2 ensures that the activity rate is in units of events$\cdot$km$^{-2}\cdot$year^{-1}.

Several kernel functions have been proposed for use in seismicity modelling, specifically the Gaussian kernel, the inverse bi-quadratic kernel and a finite kernel that vanishes at distances beyond one bandwidth. These three types of kernels are presented in Fig. 10, although this list is not comprehensive and other types might be possible.

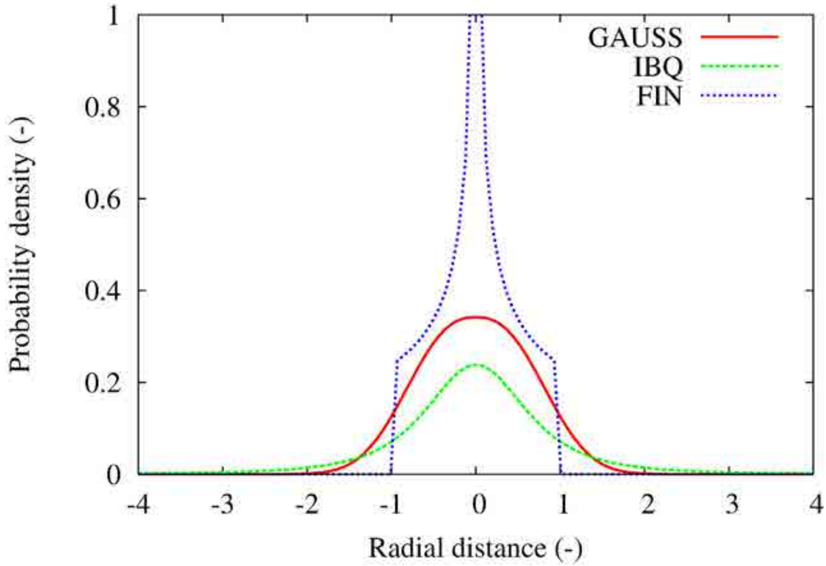

FIG. 10. Examples of unit kernel functions. GAUSS: Gaussian kernel; IBQ: inverse bi-quadratic; FIN: finite kernel. Image courtesy of M. Crespo.

3.3.3. Hybrid approaches

As explained in Section 3.3.1, the zoned approach, in its initial formulation, assigns constant activity rates to different zones. The delineation of zones in areas of low seismicity involves a certain degree of subjectivity, with different zonations being proposed by different authors for the same area. The methodology implies stepwise jumps across the zone boundaries. Several ideas have been proposed over the years to try to overcome these drawbacks. In 1986, Bender [30] introduced statistical uncertainties in the epicentre locations in order to smooth the transition of the seismic activity rate across zone boundaries. In the same year, Veneciano and Pais [31] tried to reduce the subjectivity introduced in the process of zone delineation by proposing a methodology in which the zones are automatically constructed with the sole reference of the information contained in the seismic catalogue.

Moreover, an approach that maintains some type of zonation, but takes a zoneless approach within each zone, is applied. This is the case of the methodology employed by the Electric Power Research Institute in 1986 [32], in a recently superseded United States Nuclear Regulatory Commission report issued in 2012 [33] as well as in a study by Frankel in 1995 [27].

In the Electric Power Research Institute methodology [32], GR *a*- and *b*-values may be allowed to vary spatially within each zone. Each source zone is divided into rectangular cells and the likelihood function for the GR *a*- and *b*-parameters is formulated in each cell using magnitude bins. The spatial smoothing of the *a*-parameter is achieved by multiplying the observed number of earthquakes by a normal density function. For the *b*-parameter, there may be also a smoothing, or a prior estimate can be set in order to make the GR *b*-value estimate less dependent on each zone.

In 1995, Frankel [27] proposed a methodology also based on the concept of the histogram discussed above. The geographical space where the activity rate needed to be modelled was divided into cells and the GR *a*-parameter was calculated for each of these cells, while for the *b*-value assignment, a traditional zonation was still used. However, since there is a continuous variation of the GR *a*-parameter in space, the global seismic activity rate also shows that variation. The dependence of the activity rate on magnitude still follows the GR relationship of Eq. (3) within each cell. The best known application of this this methodology is that used by Frankel [27], but others have applied it in other regions, such as in the Iberian Peninsula [34] and the Indian Peninsula [35].

Finally, the United States Nuclear Regulatory Commission's source model [33] has the same basic formulation as the model of the Electric Power Research Institute [32], but it uses penalized likelihood methodology in estimating the *a*- and *b*-values.

3.3.4. Magnitude limits used in seismic hazard studies

The integration variables of the integral from which the target motion rates are derived are magnitude and distance (see Eq. 10 in Section 3.6.1). The magnitude integration limits of this integral need to be determined.

The situation is different for the lower and upper limits. The lower limit affects only the range over which the seismic hazard results are valid, since there is no usually doubt that low magnitude events will take place. However, the decision about the maximum integration limit implies a judgement on the maximum magnitude that can actually occur, and its choice will most likely have an important influence on the hazard results of interest.

SSG-9 [1] refers to the lower magnitude integration limit in paras 5.15 and 11.17. Low return periods are mainly influenced by low magnitudes, which have a higher mean frequency of occurrence. Hence, the choice of the minimum magnitude indirectly fixes the lowest return period for which the seismic hazard curve is valid. This information should be provided together with the hazard results. The lower limit should be obtained with appropriate sensitivity analyses and, as indicated in SSG-9 [1], it should be determined by consulting the "seismic designer and/or the fragility analyst."

When deciding the lower magnitude integration limit, special attention should be paid to the magnitude range for which the GMPE is valid, since its use outside its applicable range can produce unrealistic, usually overestimated, hazard results [36]. In this respect, more recent advances in GMPE development extend the magnitude limit down to values as low as $M_W = 3$ (e.g. Ref. [37]).

From the practical point of view, if the calculation model is correct, extending the lower bound of the magnitude integration limit should not impact the higher return periods, which are usually the periods of interest for nuclear installations.

Each seismic source being used for SHA has to be assigned a maximum credible magnitude. Hazard calculations are conducted for earthquake magnitudes defined by the credible maximum magnitude in each source. The situation is that there is a mathematical representation of the seismic activity rate (the GR relation) and a decision has to be made on the validity of this representation, or, in other words, on the maximum magnitude that the seismic source will actually generate.

Several criteria for representing the maximum credible magnitude in the calculation have been used over the years. It has been very common to identify the maximum earthquake that has taken place in the region of interest and increase it by a certain quantity (e.g. half a magnitude degree, or a full degree if it is given in terms of epicentral intensity). Palaeoseismic information, where available, can be employed. The maximum magnitude will always be accompanied by an uncertainty that should be appropriately incorporated in the calculations.

There are several alternative approaches for estimating the distributions of the maximum earthquake magnitude, M_{max}, for distributed seismicity sources. The first is the Bayesian procedure, which uses the prior distributions from an earthquake catalogue that spans an extended region and that samples the largest events that have occurred in similar tectonic environments (as described in Ref. [38]). The second approach [39] uses the observed seismicity within a region to provide a direct (or posterior) assessment of M_{max}. The Bayesian approach is representative of a category of approaches that rely on drawing analogies to tectonically comparable regions in order to estimate the M_{max} for the source of interest. These approaches are based on the ergodic assumption that one can substitute time (the short period of observation) for space (other tectonically similar regions). The key difference between the Kijko approach and the Bayesian approach is that the Kijko approach does not have a prior distribution; it uses only the earthquakes within the source of interest. The prior distribution is based on analogies to other parts of the world and the assumption that those events are applicable to the estimation of maximum magnitudes within the source of interest.

The Kijko approach is representative of an alternative category of models that rely on the observation of seismicity entirely within the zone of interest. Because the occurrence of M_{max} is typically rare relative to the period of observation, these approaches assume a particular frequency distribution of earthquake sizes and, so that they can be applied with confidence to larger or very active regions, rely on significant numbers of observed earthquakes to provide stable estimates.

Both the Bayesian and Kijko approaches have their advantages and disadvantages. They both have the positive attribute that they are repeatable given the same data and that they can be readily updated given new information. The Bayesian approach is arguably more stable because of the use of a prior distribution that, even in the absence of a significant number of earthquakes in the zone of interest, can still provide a result. However, the prior distributions for M_{max} are developed based on analogies to other tectonically comparable regions, which can be a source of uncertainty, and on evaluation of those regions relative to a highly uncertain set of characteristics that are postulated to be important to M_{max}. The advantage of the Kijko approach is that it does not require the identification of analogue regions or assessments of the characteristics of those regions. However, as applied, the approach relies on the assumption that the distribution of earthquake magnitudes follows a doubly truncated exponential distribution. Moreover, the approach does not provide stable results when the number of observed earthquakes is low.

If the seismic activity rate does not have a predefined shape, but is calculated considering the individual contributions of the events, as in the kernel procedure, the maximum magnitude value is provided by the maximum magnitude included in the catalogue. Hence, in this case, the catalogue can be supplemented with events of larger magnitudes that are considered to be representative of the seismic activity that probably has not been recorded in the catalogue because of its long period or recurrence interval.

3.4. SOURCE PARAMETERS REQUIRED FOR GROUND MOTION EVALUATION

3.4.1. Source parameters for GMPEs

GMPEs are generally used for estimating ground motions from potential earthquakes. The ground motion values, such as peak ground acceleration, peak ground velocity and spectral accelerations, are represented as functions of magnitude M and distance R along with other parameters such as site amplification and source type. Ground motions recorded at a site are composed of source effects, path effects and site effects. In GMPEs, the source effects are generally represented by magnitude M and sometimes other additional parameters. In modern GMPEs, magnitude is not usually the only source parameter. The source category (Section 2.3) and focal depths are also considered in modern GMPEs as additional source parameters. Distance is also preferably measured as the shortest distance from the fault to the site, and so fault geometry determines the distance value. The path effects are primarily expressed by the distance term R, and sometimes by the seismic Q parameter along the path. The local site effects are described by a site amplification factor, G. The worldwide GMPE database edited by Douglas in 2011 [40] and the global testing results from Stewart et al. [41] are also useful references.

Some GMPEs also include forward directivity effects caused by fault rupture propagation [42] and hanging wall effects of reverse faults as source and site location parameters. Care has to be taken in specifying these source parameters when using GMPEs.

3.4.2. Source parameters for finite fault modelling

In situations where there are insufficient strong motion recordings to enable the development of reliable GMPEs, instead of adopting and adjusting GMPEs from other regions, ground motion simulations can be used. Especially in tectonically stable regions and in the near-fault environment of large earthquakes, ground motion simulations from earthquake ruptures can form the basis for the development of simulation based GMPEs. These simulations can include the effects of radiation pattern and forward directivity not explicitly considered in most GMPEs that are derived from strong motion recordings. The main parameters that are required to define a finite fault for strong motion simulation are described in Fig. 11.

Fault size is defined by length and width. Its hypocentre, strike and dip angles and depth to top of rupture are key parameters for expressing the positional relationship between the finite fault and the site. Rake angle is measured from strike direction and indicates slip direction. The radiation pattern is controlled by the fault geometry and the rake angle, and its effects are clear at long periods but become incoherent at short periods. The radiation pattern is smoothed out by averaging over data in GMPEs and by the consideration of multiple earthquake sources in PSHA.

Strike-slip faults have rake angles around 0 or 180 degrees and dip angles close to 90 degrees. Reverse faults have rake angles of around 90 degrees and dip angles of about 30 to 60 degrees. When the orientation of the regional tectonic

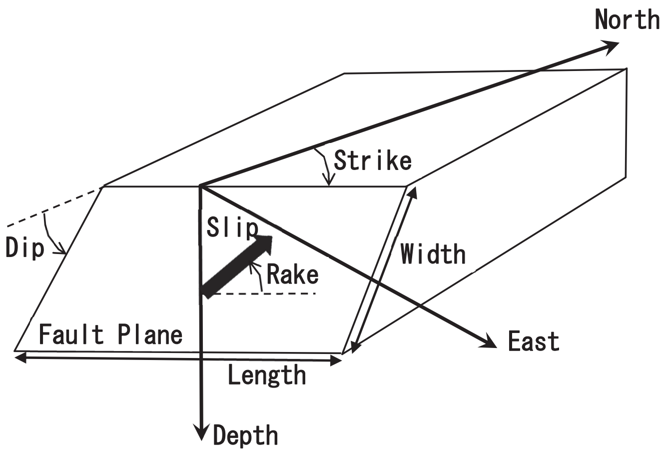

FIG. 11. Fault plane geometry, and strike, dip and rake angles of main parameters.

stress direction is defined, strike angles of reverse faults are approximately perpendicular to that direction and strike angles of strike-slip faults are oblique to that direction.

Finite fault simulations of ground motions are commonly performed for large earthquakes on identified faults in regions with mapped active faults that intersect the ground surface. In the same regions, simulations of the ground motions from smaller earthquakes occurring on unidentified faults that do not break the ground surface may also be required to treat diffuse seismicity, if it is believed that this seismicity occurs off the mapped faults. To illustrate the co-existence of earthquakes occurring on identified surface faults and earthquakes occurring on buried faults that may not have been identified, Fig. 12 shows fault ruptures of different sizes embedded in a crustal structure; these fault ruptures are not necessarily located on the same fault plane. Parameter D_1 defines the depth of the top of the fault, which is controlled by the strength of the surface rock or soils; the top of the fault tends to be shallow in stable continental regions, especially in cratons, and relatively deep in tectonically active regions. Parameter D_2 defines depth of the bottom of the fault, which is controlled by the rheology and temperature of the lower crust. The depth interval between D_1 and D_2 is defined as the seismogenic zone, within which a rupture is able to nucleate.

Figure 12 also shows that the rupture planes of smaller earthquakes are usually confined to the seismogenic zone, but larger earthquakes are able to rupture into the ductile regions (not labelled) both above and below the seismogenic zone, with slip breaking the ground surface [43]. It has been suggested that the boundary between buried and surface-breaking earthquake magnitudes in Japan is M_W 6.5 ($M_0 = 7.5 \times 10^{18}$ N·m) [7]. This magnitude threshold is derived from data in active seismic regions with large identified faults. In those regions, this suggests that even for mapped surface faults that have a very short surface fault length, the value of the maximum magnitude of surface faulting earthquakes may be as high as M_W 6.5, if no other data (such as seismicity, seismotectonic, palaeoseismic and liquefaction data) are available to constrain the maximum magnitude to lower values. It also suggests that, without data of the kinds described above, it may be difficult to exclude the possibility of earthquakes with magnitudes as large as this threshold level occurring on unidentified subsurface faults, which would then need to be treated as diffuse seismicity.

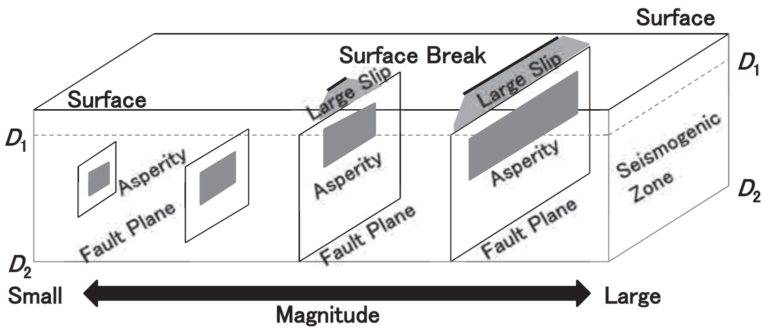

FIG. 12. Schematic diagram of buried and surface-breaking faults[43].

The parameters D_1 and D_2 depend on the tectonic environment, and need to be defined before simulating ground motions. They are usually derived from microseismic activity in the study region based on the upper and lower limits of the focal depth of earthquakes. In areas of very low seismicity, the parameters may be estimated from geophysical exploration. For example, D_1 may be taken as the depth to a P wave velocity of 6.0 km/s, and D_2 may be taken as the depth where the temperature exceeds the Curie point. In Japan, D_1 varies from about 2 to 5 km and D_2 from about 15 to 20 km, based on seismic activity and geophysical observations. The values are sensitive to the seismotectonic setting. In the cratonic regions of Australia, earthquakes as small as M 5.5 break the surface, indicating a very shallow D_1.

In tectonically stable regions with no mapped active surface faults, the seismic hazard for earthquakes of all magnitudes is sometimes based on strong ground motion simulations. These simulations are performed using hypothetical, not actual, fault models, and in this sense, they represent diffuse seismicity because the simulations are based on generic assumptions about the nature of fault ruptures in the region, not on the known characteristics of active faults that have been identified and mapped.

Figure 13 summarizes two asperity and stochastic approaches. The upper part of the figure shows the slip distribution of an earthquake derived from source inversion analysis. Stochastic source modelling, which is commonly used in the United States of America, explicitly uses this complicated slip distribution. Many fault rupture scenarios with different slip distributions are generated stochastically from the two dimensional wavenumber spectrum of the spatially varying slip, often using a k^{-2} relationship for amplitude, where k is wavenumber, based on the analysis of slip models of previous earthquakes. Hypocentres are also randomly chosen.

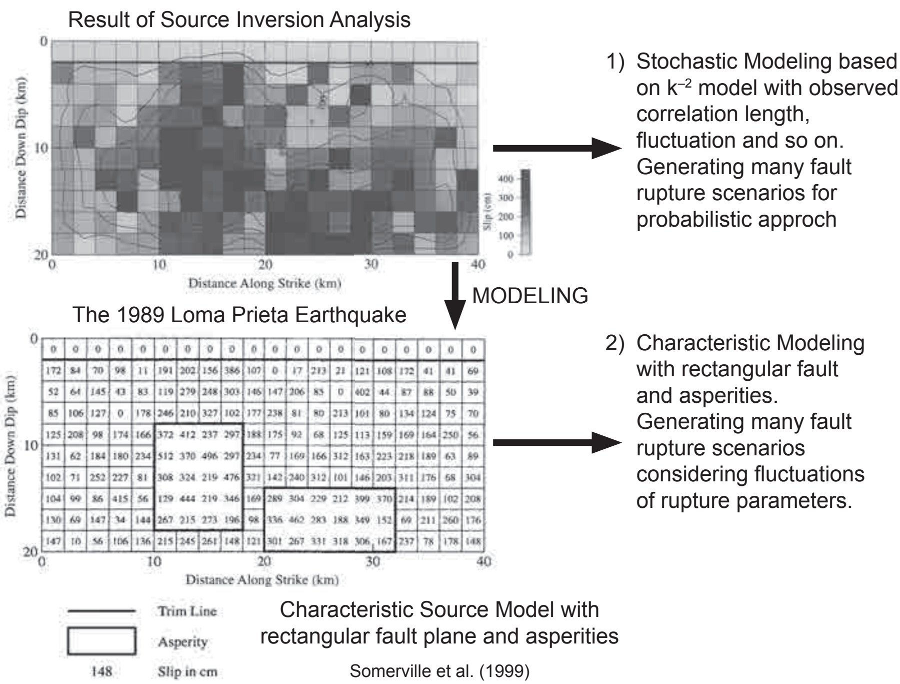

FIG. 13. Schematic diagram of stochastic and asperity finite fault models (reproduced with permission from Somerville et al. [40]; the original spelling has been retained).

In asperity modelling, which is mainly used in Japan, a simple fault model with rectangular asperities with a large slip (and strong ground motion generation area [4]) is derived from the complex slip distribution of source inversion results using a procedure for identifying asperities [43]. In this approach, many fault rupture models with different number, location and size of asperities are generated and used in simulations. The characteristic source model is a simplified representation of the real source rupture, but the simulated ground motions are validated against recordings of recent large earthquakes in Japan and elsewhere; this is effective in modelling forward directivity effects. Forward directivity effects can generate large ground motions even in moderate earthquakes; for example, a peak ground acceleration over 1g was observed in an M 6.1 earthquake in December 2004 at the K-NET HKD020 station, a hard sediment site in Rumoi, Hokkaido, Japan [44]. This indicates the relevance of fault rupture modelling for identified faults, and suggests that it should also be considered in the case of diffuse seismicity.

3.5. GROUND MOTION EVALUATION

To evaluate ground motions at a site, previously recorded ground motion data provide an important frame of reference. Ideally, ground motion information would include data from earthquakes with approximately the same magnitude and fault mechanism recorded on similar site characteristics with similar source-station geometry. However, especially in regions of diffuse seismicity, adequate strong ground motion data from past large earthquakes do not exist. Such information can be derived from global strong motion databases or from appropriate site specific strong motion simulations. The expected levels of ground motion from possible future earthquakes may therefore need to be estimated largely using simulations.

3.5.1. GMPE and site response considerations

GMPEs provide initial estimates of ground motion characteristics that can be expected at a site from a specified scenario earthquake.

The applicable ranges of magnitude and distance in the GMPEs are controlled by the database. Since GMPEs employ different distance definitions, such as epicentral distance, Joyner and Boore distance, and so on, care has to be taken in using them for ground motion evaluation.

Ideally, local GMPEs that reflect the local seismotectonic setting at the site should be used, since GMPEs are region specific. In addition, local site conditions have a significant impact on ground motion levels, which is why most GMPEs are specified for a given site condition or have site condition as a variable. Adjustment of GMPEs from a site condition to the conditions observed at the site of interest may result in more reliable estimates with residual differences between the observed values and those predicted by GMPE, although the estimates may not fulfill the requirements of a site specific ground motion study. Further, the appropriateness of GMPEs based on data that are from outside the site region of interest should be studied by comparing GMPE predictions with available data from the site or site region.

3.5.2. Strong motion simulations

Ground motion simulation based on fault rupture modelling is used for directly estimating the ground motions for scenario earthquakes in scenario based SHA, and for generating ground motions in situations where few strong motion recordings are available.

The applicability of GMPEs is limited by the distribution of magnitude, distances and site conditions contained in the databases from which they are constructed. In order to reduce these limitations, especially in tectonically stable regions or in the near-source region of specific fault geometries, ground motion simulations can be used to augment the recorded data using procedures that have been validated against relevant recorded ground motions. Simulations can be performed for many different rupture propagation scenarios and many different geometrical relationships between the site and the fault, thereby helping to reduce the limitations in the recorded strong motion database. Especially in tectonically stable regions and in the near-fault environment of large earthquakes, ground motion simulations from earthquake ruptures can also form the basis for the development of simulation based GMPEs. However, uncertainties may arise when it is necessary to apply simulations to earthquake magnitudes and source site geometries that lie outside the conditions for which it has been possible to validate them against recorded data. Such simulations have been used in several tectonic environments, including in stable continental regions and near-source regions [45]. Examples of the application of these kinds of simulations are provided in Section 3.6.3 and 4.2.

3.5.3. Comparable scenario recordings

An alternative to the use of GMPEs based on strong motion recordings is to find the upper bound from the spectra of the compilation of strong motion recordings of comparable earthquakes, that is, earthquakes that are categorized as diffuse seismicity in the appropriate tectonic setting. In Japan, this category has sometimes been defined on the sole basis of an upper magnitude threshold (e.g. in Ref. [7]) combined with a lack of field evidence for surface rupture in the event. A more complete definition of diffuse events would include consideration of whether the event occurred on an identified fault, regardless of whether it broke the ground surface. The advantage of this approach, which is usually used in situations where few recordings are available, is that it provides for a detailed consideration of all of the available recordings, which contain aspects that reflect source rupture processes, propagation path effects and local site effects. This approach is particularly important in the near-fault environment where recordings are sparse but have important implications for the largest ground motions that are expected from a maximum earthquake magnitude. The spectra of the recordings may be used as a reference for establishing the design spectrum. However, a single record does not have the largest amplitudes at all periods, and there might have been larger amplitude ground motions at locations where there were no recording stations. Moreover, larger earthquakes may have happened in the past or may be possible in the future. To accommodate these concerns, spectra of several different earthquake events and different site conditions are considered for hazard evaluation. The collection of source, path and site effects is required before combining records from the different events, because the records vary with the earthquake source, path and site conditions.

An example of this kind of design spectrum in Japan is shown in Fig. 14. On the left panel, dashed lines are response spectra, after site corrections, of seven observed ground motions from worldwide earthquakes that occurred on unidentified faults. The red line shows a design spectrum that envelopes the observed spectra (this spectrum is known as Kato's Spectrum) [46]. The right figure shows site corrections of the design spectra [47]. Since Japan is located in one of the most seismically active regions, the largest earthquake records from unidentified faults are used to define minimum design spectra. This kind

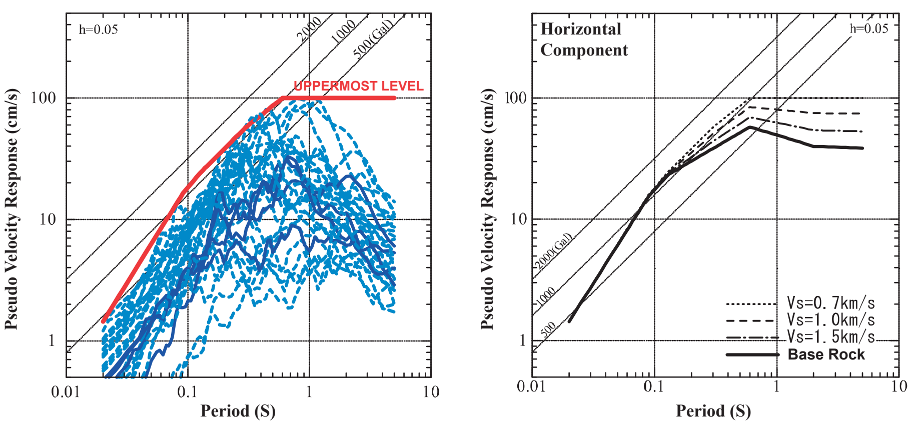

FIG. 14. An example of a design spectrum that envelopes recorded near-fault spectra from worldwide earthquakes that occurred on unidentified faults (left, M_W 5.6–6.6, distance to fault 3–17km) and its site corrections (right) [46].

of observation based design spectrum can be used as a minimum requirement for addressing diffuse seismicity.

This approach differs from the GMPE approach, in which the model provides a direct estimate of the ground motion level, including its median expected value and random variability. In that sense, the GMPE provides a more rigorous estimate of the expected ground motion level. However, in situations where data are sparse, which may include stable continental regions and the near-fault environment in tectonically active regions, the GMPE approach may be subject to a large degree of uncertainty. In these situations, there may be some advantage to be gained by using the analysis of a global set of recorded spectra as described above. The main shortcoming of this approach is that it does not provide a clear methodology for assessing the uncertainty in the ground motion estimate.

In Japan, M_W 6.5 or larger represents the largest diffuse earthquake magnitude because the area is tectonically very active. In applying the approach to other regions, the maximum magnitude of diffuse seismicity should be based on expert judgement using historical, tectonic and palaeoseismological evidence. Appropriate recorded ground motions should be selected from worldwide databases to define a minimum design spectrum.

3.6. HAZARD ASSESSMENT

3.6.1. Probabilistic SHA

In probabilistic SHA, the annual frequency of exceedance is calculated by integrating the contributions from all faults or seismic sources as follows:

$$\Phi(s) = \sum_{i=1}^{Faults} \left(\iint_{m,r} f(m)(P(SA > s|m,r)P(r|m)dmdr \right)_i \tag{10}$$

where

$f(m)$ is the probability density function for rate of events of magnitude m;

$P(SA > s|m,r)$ is the probability that spectral acceleration, SA, exceeds a specified level for a given magnitude m and distance r;

$P(r|m)$ is the probability that the source to site distance is r, given a source of magnitude m.

The location of diffuse seismicity sources and the sizes of the maximum earthquakes that are assigned to it are important for PSHA, but their influence on the calculated ground motions is not as strong as in scenario based SHA. This is because the ground motion hazard contains contributions from earthquakes of all magnitudes occurring on all of the earthquake sources that can affect the site, and those contributions take account of the random variability in ground motion level for a given earthquake magnitude and distance. Three reasons for the relative insensitivity of probabilistic SHA to the characterization of diffuse seismicity, compared with the case of scenario based SHA, can be identified. Some of the critical parameters needed to conduct a probabilistic SHA are described below.

3.6.1.1. Maximum magnitude

In regions of very low seismicity, when the largest earthquakes have recurrence intervals that are much longer than the time period of interest, then the hazard is dominated by earthquakes whose magnitudes are less than the maximum magnitude that is assigned to the seismic source. While the selection of the maximum magnitude is important and may have a significant impact on the hazard, it is less critical than in the case of scenario based SHA, but the frequency of occurrence of smaller earthquakes becomes important.

3.6.1.2. Source location

Probabilistic SHA takes account of earthquakes occurring on all of the earthquake sources that can affect the site, including both nearby and distant sources. In regions where the identified seismogenic structures are located at some distance from the site, the diffuse seismicity in the region around the site is commonly represented by a zone of uniformly distributed seismicity, and the probabilistic SHA contains contributions from the whole zone surrounding the site, not just from the part of the zone that is closest to the site. Consequently, the precise location of the zone, which in the scenario based approach may be specified by the shallowest depth of the zone beneath the site, has less impact in the probabilistic SHA approach.

3.6.1.3. Epsilon

Epsilon is defined as the fractional number of standard deviations by which a given ground motion level differs from the median ground motion level that is predicted by a GMPE or by a ground motion simulation procedure for a specified earthquake magnitude and closest distance. In probabilistic SHA, the seismic hazard is integrated over the random distribution of ground motion level.

Consequently, the ground motions from a distant source can potentially exceed a given ground motion level at a site more often than the ground motions from a nearby source, if the distant source has more frequent earthquakes than the nearby source. This may be true even if the distant and nearby sources have the same maximum magnitude. This is because the larger frequency of earthquakes on the distant source may give rise to the random occurrence of high epsilon values more often than the infrequent earthquakes on the nearby source. In scenario based SHA, epsilon is usually assigned a fixed value (such as 0 for the median level or 1 for the 84^{th} percentile level) that is the same for all earthquake sources, and so earthquake frequency is not a consideration, and the outcome is controlled solely by the combination of magnitude and distance that gives the highest ground motion level for a fixed value of epsilon.

3.6.2. Scenario based SHA

In scenario based SHA, the hazard level is controlled solely by the combination of magnitude and distance that gives the highest ground motion level for a fixed value of epsilon. Consequently, in scenario based SHA, although the seismic hazard level is independent of the rate of the seismicity because it uses a fixed value of epsilon, it is extremely sensitive to the maximum magnitude and location of the diffuse seismicity, for the reasons described in Sections 3.6.2.1–3.6.2.3.

3.6.2.1. Maximum magnitude

In scenario based SHA, the ground motion hazard level from diffuse seismicity is usually controlled by the magnitude of the largest earthquake that is expected to occur in the diffuse zone that lies closest to the site, and no consideration is given to how infrequently an earthquake of that magnitude can occur. Consequently, the seismic hazard is very sensitive to the selection of the maximum earthquake magnitude.

3.6.2.2. Source location

In scenario based SHA, the ground motion hazard level from diffuse seismicity is usually controlled by the proximity of the maximum magnitude event to the site. Consequently, the seismic hazard is very sensitive to the location of the diffuse seismicity with respect to the site. The proximity may be controlled by the shallowest depth of the diffuse seismicity, and the seismicity may be assumed to occur directly beneath the site, even though the probability of occurrence of such an event may be very low.

3.6.2.3. Epsilon

In scenario based SHA, epsilon is usually assigned a fixed value (such as 0 for the median level or 1 for the 84th percentile level), and the frequency of occurrence of the earthquake is not a consideration. The hazard level is controlled solely by the combination of magnitude and distance that gives the highest ground motion level for a fixed value of epsilon.

3.6.3. Simulation based probabilistic SHA

Empirical GMPEs are most frequently used for evaluating ground motions in probabilistic SHA (PSHA) because of their ease of use. However, they are subject to a large degree of random variability due to source dependent randomness and fluctuations caused by path and site effects. From recent damaging earthquakes, it is clear that source conditions such as the locations of asperities and the hypocentre result in large variations in ground motions, particularly in the near-source region. Ground motions estimated by fault rupture modelling naturally include these source effects, and also have the advantage of generating waveforms from which any kind of ground motion parameter can be derived. Ground motion simulations are usually used in a limited number of scenarios, but they have also been applied in PSHA [48]. Fault rupture modelling for SHA is expected to provide more site specific and realistic estimates of the hazard than those which are obtained by using empirical GMPEs, if the source and fault parameters are known.

Figure 15 shows an example of randomly generated earthquake fault rupture scenarios. Each fault has an individual source rupture scenario with an asperity source model. This kind of calculation can also address two other situations: one in which mapped surface active faults are very short and the magnitude of the maximum earthquake is uncertain, and another in which smaller magnitude diffuse earthquakes associated with an identified active fault need to be evaluated.

In order to provide a realistic representation of variability in the simulated ground motions, it is important to use appropriate distributions of the random values of the parameters that control the rupture scenarios. It is especially important to avoid the double counting of correlated parameters, because this results in the accumulation of a large and unrealistic degree of random variation. The Appendix explains how these results are used to estimate ground motions with a specified probability of exceedance.

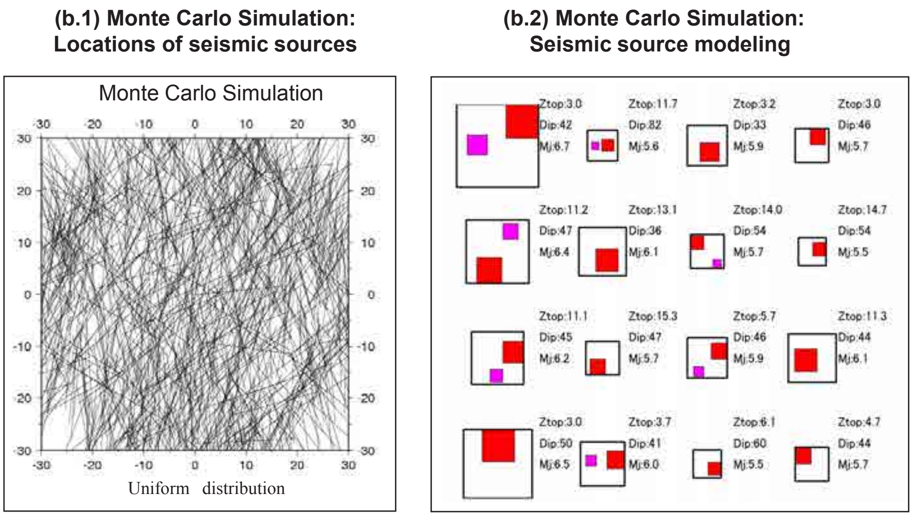

FIG. 15. Randomly generated fault rupture scenarios around a site (image courtesy of the Japan Nuclear Energy Safety Organization (JNES)).

3.7. TREATMENT OF UNCERTAINTIES

Uncertainty in the evaluation of ground motion consists of epistemic uncertainty and aleatory variability, as described in SSG-9 [1]. The following subsections form a practical description of both types; the combination and distinction of both types needs to be considered.

3.7.1. Epistemic uncertainty

Epistemic uncertainty is uncertainty about the true state of nature. Therefore, alternative models are mutually exclusive. Examples of epistemic uncertainty are the length and dip angle, slip rate and maximum magnitude of a fault, and the relationships between earthquake source and ground motion parameters embodied in GMPEs. Epistemic uncertainty can, in principle, be reduced by gathering data. Whenever these uncertainties are large enough to have a significant impact on the calculated seismic hazard level, consideration of all the viable alternative models is required. For nuclear installation projects, epistemic uncertainty is reflected in a range of viable models, multiple expert interpretations and statistical confidence (see SSG-9 [1]) to weigh the alternative models. Epistemic uncertainty gives rise to uncertainty in the true value of the mean hazard, as shown in Table 1.

TABLE 1. PARAMETERS THAT DESCRIBE EPISTEMIC UNCERTAINTY AND RANDOM VARIABILITY IN SHA

	Central value	Random (aleatory) variability of central value
Best estimate	Median (μ)	Sigma (σ)
Epistemic uncertainty in true value of best estimate (standard error of best estimate)	σ_{μ}	σ_{σ}

Treatment of epistemic uncertainty occurs outside the hazard integral to probabilistic SHA. In both scenario based and probabilistic SHA, logic trees with appropriate weights are used to address the epistemic uncertainty, which is represented by alternative models. In probabilistic SHA, median and fractiles of the resulting hazard curves can be developed in addition to the mean hazard curve. The fractiles of the hazard show the uncertainty in the true value of the mean hazard for a specified annual probability of exceedance. The usual practice is to use the mean response spectrum, but higher fractiles may be used in risk based assessment.

3.7.2. Aleatory variability

Aleatory (random) variability is event-to-event variability about a median value. Alternatives exist together. Examples include the depth and rupture area of an earthquake of a given magnitude, and the variability in ground motion level recorded at stations located at the same distance from the same earthquake. It cannot be reduced by gathering more data, although additional data may provide more accurate quantification, which is performed by measuring the standard deviation of the random variations in data sets. Aleatory variability causes the hazard level to increase with increasing return period. It does not necessarily give rise to uncertainty in the true value of the mean hazard.

In probabilistic SHA, aleatory variability in ground motion level is treated by integrating over the random variation in epsilon (the number of standard deviations away from the median level) of the GMPE within the hazard integral. This is automatically included in the hazard curves produced by probabilistic SHA. Additional random variability in ground motion levels due to random variations in hypocentre location is used in the modelling of rupture directivity effects, which depend on the location of the hypocentre. In scenario based SHA, aleatory (random) variability is treated differently: it requires a policy decision on ε (the number of σ away from the median) used to define the ground motion level.

The treatment of aleatory variability can change as more information about an earthquake source becomes available, or as more predictive variables are included in GMPEs. For example, GMPEs did not originally consider hanging wall effects, which are now known to cause spatial variations in ground motion levels recorded at the same distance from an earthquake. Variability in ground motion level previously considered to be random can now be properly attributed to hanging wall effects, and skilful inclusion of a hanging wall term in the GMPE will result in reduction of that component of aleatory variability and reduction in the overall level of aleatory variability. However, if the site is located on the hanging wall of the fault, the median value of the ground motion may increase owing to hanging wall effects.

Another advance in the treatment of aleatory variability is the estimation of single station sigma, which is the random variability in ground motion level that is observed at a single recording site [49–52]. Single station sigma is found to be significantly lower than the total sigma that is conventionally used, because total sigma includes the station-to-station variability in site response for a specified source category (as defined by the average shear velocity down to 30 m, V_{s30}, or a geological site classification). Since the focus of SHA for nuclear installations is on a single site, single station sigma is potentially highly relevant to nuclear installations, and the measurement of single station sigma at the site should be a high priority at any nuclear installation, and could also be used in site selection.

From recent damaging earthquakes, it has become clear that random variations in source conditions such as the locations of asperities and the hypocentre result in large variations in ground motion levels, particularly in the near-source region. Ground motions estimated by fault rupture modelling naturally include the effect of source conditions, and provide waveforms from which any desired ground motion characteristics can be derived. Fault rupture modelling for scenario based SHA is quite feasible because it requires the modelling of relatively few scenarios, and provides more realistic ground motion estimates than are available from GMPEs. It is also feasible in PSHA [48], although it requires large computational resources.

The parameters used in such ground motion simulations have individual distributions that need to be appropriately modelled by a median value and its standard deviation. Fault rupture modelling involves the use of many different source parameters. If the standard deviation of each parameter is overestimated, or if the relationships between the different parameters are not considered, then a very large degree of random variability may accumulate. Simulations with appropriate modelling of parameters should correspond to evaluations using GMPEs and to observed data. As mentioned above, Fig. 15 shows an example of randomly generated earthquake fault rupture scenarios. Each fault has a different rupture scenario represented by an asperity model. The resulting ground motions should be tested against GMPEs and observed data.

When fault rupture models are used to estimate ground motions, the total uncertainty is partitioned in a manner that is different from the epistemic-aleatory partition [53]. Modelling uncertainty, measured by the difference between recorded and simulated ground motions, represents the discrepancy between the actual physical processes and the simplified representation of them in the model [54]. Parametric uncertainty represents the uncertainty in the values of the model parameters in future earthquakes [54]. The total uncertainty is obtained from the combination of these two components. These two different partitions of uncertainty are represented in matrix form in Table 2.

TABLE 2. PARTITION OF UNCERTAINTY IN GROUND MOTION PREDICTION MODELS [52]

	Epistemic (σ_μ, σ_σ)	Aleatory (σ)
Modelling	σ_μ: Uncertainty in the true bias of the model σ_σ : Uncertainty in estimate of σ_{m}	σ_{m}: Unexplained scatter due to physical processes not included in the model
Parametric	σ_μ: Uncertainty in median values of source and path parameters σ_σ : Uncertainty in probability distributions of parameters	σ_{p}: Event-to-event variation in source and path specific parameters of the model

In 2013, Cotton et al. [55] pointed out that the variability of stress drop strongly affects the distribution of simulated ground motions, and that the random variability in stress drop derived from source studies results in larger random variability in ground motion level than is present in observed ground motion data and GMPEs. Further study on the random variability of stress drop that is appropriate for fault rupture modelling is required to reduce the unrealistically large variability of ground motion levels that they may produce.

Fault rupture modelling to address random variability in probabilistic SHA is less feasible because it requires the modelling of many scenarios, but it has been done in research-based applications [48].

3.8. COMPARISON OF METHODOLOGIES

In this section, different approaches to performing a PSHA are compared. The comparison is not comprehensive, but tries to highlight the main aspects that can help with the understanding as well as the selection of the methodology.

As indicated in Section 3, the various tasks performed in an SHA can be divided into the following groups:

(1) Compilation of the seismic catalogue;
(2) Construction of the seismic source model;
(3) Selection of appropriate GMPEs and/or simulation approaches;
(4) Combination of the seismic source model and the GMPEs or the simulation approach;
(5) Derivation of the hazard.

The main differences between the methodologies for performing a PSHA are in the way that the seismic source model is constructed and how the seismic activity is translated into ground motion by means of a GMPE or by performing simulations. There may be also some differences related to point (1) above, namely the information needed for each event in the catalogue or the operations to be performed on it.

Concerning the catalogue, there is some basic information that is needed for each earthquake listed regardless of the methodology, such as the location and magnitude of the earthquakes. Uncertainties for each of these parameters should also be documented, but the way in which they are incorporated in the calculation varies for each methodology. When employing the GR relation, all the event uncertainties within a zone (or a cell, in the Frankel approach [27]) are translated into two uncertainties, mainly those associated with the GR *a*- and *b*-parameters. Additionally, not all computational codes allow for the incorporation of such uncertainties. In this case, the only way to account for them would be via a logic tree approach. However, in cases where each event contributes independently to the construction of the activity rate, uncertainties on the location and magnitude are incorporated on an event-by-event basis, allowing the corresponding variables to adopt a certain probability distribution around the values in the catalogue.

The homogenization of the catalogue in terms of the chosen magnitude (see Section 3.2.2) or its declustering (see Section 3.2.3) are activities common to all methodologies. The extent of effort also varies in seismic source characterization depending on the choice of either zoned or zoneless approaches. In the zoneless approach, a decision on the model parameters that control the spatial extension of each unit function has to be made. Similarly, in the hybrid approaches, both seismic source characterization and seismic model parameterization smoothing functions need to be determined.

Finally, in the hybrid approaches, the size of the cells into which the space is divided is also an element of decision. Generally, the selected cell size is much smaller than the typical distance covered by the smoothing functions so its impact on the results is much smaller than the size of the smoothing function.

When constructing the seismic activity rate, the completeness years are needed and only those earthquakes that occurred after these years are considered for the computation of the GR *a*- and *b*-parameters. However, when the seismic source is constructed as a sum of individual contributions from the events, no event should be discarded. This is because the elimination of certain events would result in a loss of information on the spatial distribution of the seismic activity.

In the selection of the maximum magnitude for a seismic source, the earthquake catalogue may need to be supplemented with additional events in diffuse seismicity regions, because large magnitude earthquakes may not be represented well in the catalogue, but this can be adjusted using geological and/or palaeoseismic studies. The selection of the minimum magnitude for integration is common to all the methodologies.

4. EXPERIENCES IN SEISMIC HAZARD ASSESSMENT FOR DIFFUSE SEISMICITY

4.1. UNITED STATES OF AMERICA

This section describes representative approaches that have been developed and applied in the USA[1]. Some aspects of these approaches may be specific to the tectonic conditions within the USA and to the kinds of data that are available; hence, they may not be generically applicable. They are provided to illustrate the choice of methodologies available for use. The following summary is drawn from the Central and Eastern United States Seismic Source Characterization (CEUS-SSC) study [33].

In SHA, diffuse seismicity is represented by distributed earthquake sources, using either source zones or a zoneless approach (Section 3.3). In regions of

[1] This section is based on Ref. [30]

low seismicity, patterns of diffuse seismicity are defined from generally small to moderate magnitude earthquakes that have occurred during a relatively short (i.e. relative to the repeat times of large events) historical and instrumental record. Therefore, the locations of future events are not as well constrained by the locations of past events as more seismically active identified seismotectonic structures are.

SHA studies employed in the USA for nuclear installations generally use a truncated GR relation with variable *a*- and *b*-values within each designated seismic source. A degree of spatial smoothing is also applied. The spatial smoothing operation is typically based on calculations of earthquake recurrence within one quarter degree or one half degree with allowance for correlation between the cells. Both *a*- and *b*-values are allowed to vary, but the degree of variation is optimized so that *b*-values vary little across the study region. A balance is struck between variations in *a*-values that are too sharp, reflecting a reliance on the exact locations and rate densities of observed events that is too strong, and variations that are too smooth, reflecting an unwarranted belief that the observed record does not provide a spatial constraint on rate density variation.

The seismicity is modelled using a dense grid of point sources for magnitudes below a certain threshold. Above that magnitude threshold, the seismicity may be modelled by a dense grid of lines or planes, which requires some assumptions about the strike and style of faulting of the earthquakes. The depth distribution of the seismicity is described in the established source models. Geological, geophysical and seismicity data from the site region may be used to further constrain the depth of seismicity.

In the remainder of this section, the implementation of these approaches in the central and eastern USA is described. This is an intra-plate region characterized by a low to moderate level of seismic activity. In the CEUS SSC study [33], two categories of earthquake sources are considered. The first is repeated large magnitude earthquake (RLME) sources identified based on well defined evidence for Late Quaternary or Holocene RLMEs. The second category comprises background zones, which cover all other areas without any identifiable fault sources. Some of the RLME sources are treated as seismotectonic structures, and characterized by slip rates and recurrence intervals on identified faults, but others are treated as distributed seismic source zones representing diffuse seismicity.

RLME sources and background zones are parts of the unified source model. The background sources are further split into two separate source types: M_{max} zones and seismotectonic sources. The M_{max} zones model involves the assumption that there is limited information about the seismic sources in the region and only limited tectonic information is used to define the region. The CEUS study region is subdivided according to whether or not there is evidence of Mesozoic and younger extension (with associated uncertainties in the location of the boundary). In this model, the spatial variation of recurrence parameters is based on spatial smoothing of observed earthquakes. The spatial smoothing is typically done over one quarter or one half degree cells. The maximum magnitude assignments follow a process described in Section 3.3.4.

The seismotectonic source portion of the model includes several sources developed using current knowledge of geological characteristics. Differences in the style of faulting, strike of ruptures and depth distribution of future earthquakes are accommodated in the seismotectonic model. The model also accommodates any differences in maximum magnitudes determined based on the largest observed earthquakes in each zone or its global equivalent.

The weights assigned to the M_{max} zone and seismotectonic zone branches reflect the relative preference for the alternative approaches to characterizing the future spatial and temporal distribution of earthquakes and their characteristics, given the available data for the CEUS. The two models are quite similar in many respects. They both include RLME sources as independent sources defined by palaeoseismic evidence for the size and recurrence rate of RLMEs. Moreover, both allow spatial variation of recurrence parameters by smoothing within seismic source zones. The key difference between the two models is in their ability to include and represent information related to the characteristics of future earthquakes. The M_{max} zones model is based on average or default characteristics that are representative of the entire study region, whereas the seismotectonic zones model can include information that allows for an assessment of spatial variations of future earthquake characteristics at a scale that is appropriate to a regional SSC model. While many of the characteristics of the seismotectonic zones are uncertain, such as the locations of the source boundaries and the characteristics of future earthquake ruptures, they are still judged to provide a better description of the applicable source characteristics and are given a higher weight in seismic hazard calculations. The CEUS model is used as a starting point for all seismic hazard studies of nuclear power plants (NPPs) in the central and eastern USA.

4.2. JAPAN

In Japan, particular attention has been paid to seismic issues in the location, design and construction of NPPs, because of high seismicity. A former regulatory guide issued by the Atomic Energy Commission in 1978 [56] required the formulation of two levels of design basis ground motions (DBGM), i.e. S1 for the maximum earthquake and S2 for the extreme case; the latter was used for the seismic design of important safety related structures, systems and components.

The Nuclear Safety Commission revised the guide in 2006, integrating S1 and S2 into a single level (known as the DBGM Ss). In detail, the 2006 guide [57] and a 2013 regulatory guide issued by the Nuclear Regulation Authority [58] required that the DBGM Ss should be determined by considering the following two types of ground motions, 'site-specific ground motions formulated by specifying seismic sources' and 'ground motions formulated without specifying seismic sources'. This treatment is comparable with the consideration of the two types of seismic sources in the IAEA Safety Guide SSG-9 [1] as described in Section 2.1.

In the case of inland crustal earthquakes, there are always some seismic sources that are difficult to identify in advance, even by implementing detailed surveys (e.g. geomorphological survey by using aerial photographs or geological field survey). By using the seismogenic source model (e.g. Ref. [7]), inland crustal events are classified into three categories as shown in Fig. 16. Category I earthquakes are those whose ruptures are always confined in the seismogenic layer, e.g. in blind faults. Category II earthquakes are those with short fault traces, which are therefore more likely to be overlooked. Category III earthquakes are those with clear fault traces which can be identified in advance. Category I and category II earthquakes are the target events without specifying seismic sources in Japan.

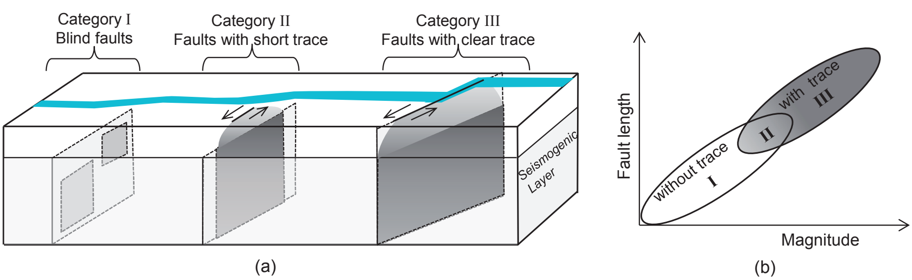

FIG. 16. Source categorization and targeted crustal earthquakes (Category I and II). (a) Categorization of crustal earthquakes based on the seismogenic layer model. (b) Relationship between fault length and magnitude.

By collecting near-source strong motion data recorded from inland crustal earthquakes and analysing the identifiability of their sources based on geological surveys, in 2004 Kato et al. [46] proposed a response spectrum (known as Kato's Spectrum, see Section 3.5.3) as the upper level of strong motions for earthquakes whose sources it is difficult to specify in advance. Kato's Spectrum has been used by utilities to develop the DBGM Ss to meet the requirement of considering ‘ground motion evaluated without specifying seismic sources’. The so-called upper level, however, is challenged by the stability problem because of the limited availability of the observation data at the time. It is necessary to re-examine its validity against new observation data.

In contrast to the deterministic method applied by Kato et al. [46], the Japan Nuclear Energy Safety Organization (JNES) proposed a probabilistic approach to address the development of ground motions evaluated without specifying seismic sources [59, 60]. In the works, they generated many combinations of a few dozen fault models and a few hundred site locations, and simulated ground motions by using the fault modelling method. From the simulated ground motions, seismic hazards such as uniform hazard response spectra (UHRS) were assessed as shown in the Appendix.

4.3. EUROPE

This section describes different approaches to SHA for nuclear installations that have been applied in different countries in Europe (for instance, France, Germany and Switzerland). The example cases provided are certainly not exhaustive, and other European countries might have used similar or different approaches depending on the regulatory framework of the country.

4.3.1. France

In France, the seismic risk for nuclear safety is guided by a site specific deterministic approach. The full methodology is published and accessible on the web site of the French Safety Authority [61]. The deterministic methodology is based on the selection of seismic scenarios. The methodology can be summarized in six main steps:

(1) Determine the seismotectonic zonation, based on geological and seismological criteria; each zone is considered to have a homogeneous seismic potential.
(2) Estimate of the characteristics of the historical and instrumental events that occurred in these seismotectonic zones. It is assumed that historical earthquakes are likely to reoccur in the future, with an epicentre in the most penalizing position for the site of interest.
(3) Retain, for the considered site, one or more events that produce the most penalizing effect (in terms of intensity at the site). In other words, the

events are moved inside the zone they belong to as close as possible to the site, and they constitute the maximum historically probable earthquake.

(4) Associate a safe shutdown earthquake to each maximum historically probable earthquake, which is obtained by increasing the maximum historically probable earthquake magnitude by 0.5 corresponding to an increase of 1 degree in intensity.

(5) Perform a site effect study to characterize geotechnical and geological material properties. The methodology distinguishes two site classes using the V_{s30} parameter, and models the geology as a 1-D structure. In case of site effects due to geometrical and/or rheological configurations, a specific study has to be performed.

(6) Evaluate the seismic motion (mean acceleration response spectra) related to the safe shutdown earthquake using an attenuation relationship (in France, the attenuation relationship of Berge-Thierry et al. [62] is used). The attenuation relationship predicts, for a magnitude and distance couple, a pseudo-acceleration value for a frequency range, accounting for the site condition (rock or soil).

If any credible palaeoseismic evidence exists near the site, the associated seismic motion at the site has to be assessed, and compared to the safe shutdown earthquake motion. Finally, the methodology requires the verification of the level of the safe shutdown earthquake and palaeoseismic events with respect to a minimal response spectrum (defined for the two soil conditions) with a peak ground acceleration set at 0.1g. The minimal response spectrum is an envelope spectrum of two: a large event of 6.5 magnitude located at 40 km from the site, and a local one of magnitude 4.5 at 10 km from the site. This minimal reference is used to design structures in cases where the seismic hazard is assessed as very low. This minimal level was introduced in order to conform with IAEA recommendations (section 2.10 and 2.11 of SSG-9 [1]) and to reduce inconsistencies in the assessment of hazard in low seismicity areas.

The application of this methodology by different experts can lead to different analysis results. This fact is clearly related to the interpretation of the data and the way in which final hypotheses are chosen with respect to the uncertainties. Each step of the methodology is then crucial, and the first two are particularly so. These are seismotectonic zonation and characterization (in terms of intensity, magnitude, and depth) of known seismicity, because they contribute to the choice of the site reference scenarios.

Owing to limited knowledge of probable active structures, and especially to the lack of a clear correlation between earthquakes and identified faults, the modelling of seismic motion in the framework of regulation is simplified. The simplification corresponds to considering (a) the seismic source as a point source; (b) the seismic energy through a single parameter, which is the magnitude; (c) the wave propagation through a single parameter, which is the distance; and (d) the site geotechnical characteristics through a site coefficient valid only for 1-D geometry. The seismic motion is then evaluated using an empirical attenuation relationship. It means that complex source effects due to the extended fault plane are not explicitly accounted for. Baumont et al. [63] studied this topic, considering a case in France of a well identified seismic source to which historical and instrumental earthquakes are clearly associated and testing this simplification. The performed tests exhibited a reasonable conservatism of the approach with respect to scenarios accounting for all source complexities (e.g. extended source, broadband dislocation on fault, focal mechanism, variable rupture velocity and directivity effects).

Local site effects are accounted for in the methodology by a site coefficient in the strong motion attenuation relation prediction. This approach is valid only for simple geometry sites, i.e. sites presenting only vertical rheological shear wave velocity variation. Based on the V_{s30} parameter, two site categories are defined: rock sites with a V_{s30} greater than 800 m/s, and soil sites with a V_{s30} between 300 m/s and 800 m/s. The methodology stipulates that for low velocity sites (e.g. lower than 300 m/s) and for complex site geometries (e.g. 2-D and/or 3-D), a specific site study is required.

4.3.2. Germany

In Germany, according to the national regulation for the design of NPPs against seismic events [64], a deterministic (scenario based) SHA and a PSHA have to be performed. The applied scenario based approach is in compliance with the recommendations in SSG-9 [1] and is similar to the French approach. In practice, the PSHA follows the traditional approaches to diffuse seismicity using seismic source zones. Uncertainties have to be considered in both approaches. The final results in terms of response spectra from the scenario based hazard assessment and the PSHA have to be compared. Possible differences between both results have to be explained, before the final elastic design spectrum for an annual probability of 10^{-5} is determined. Besides the evaluation of ground motion in terms of response spectra for the site, a design intensity also has to be evaluated. Owing to the parallel use of magnitudes and intensities, in practice, empirical GMPEs as well as intensity based attenuation equations are used. In some studies, an evaluation of strong motion registrations is used in addition to GMPEs to calculate response spectra for controlling earthquake scenarios. In cases where significant site effects are expected, soil dynamic calculations are performed in addition to the seismic hazard calculation to increase the precision of the response spectra. Furthermore, a disaggregation analysis is needed.

4.3.3. Switzerland

In Switzerland, the regulation was changed from the deterministic approach to a fully probabilistic approach in 2009 [65]. Their probabilistic safety assessment (PSA) includes a PSHA, a probabilistic evaluation of seismic fragilities and an analysis of earthquake accident sequences. For vibratory ground motions caused by earthquakes, a detailed probabilistic assessment is required.

In order to address this regulatory requirement, Swiss NPPs have taken part in the Probabilistic Seismic Hazard Analysis for Swiss Nuclear Power Plant Sites (PEGASOS) [66] and in the PEGASOS Refinement Project [67]. These studies are based on a systematic expert assessment of all available data and models integrated into a logic tree approach. A key aspect of the studies was the systematic quantification of the aleatory variability and epistemic uncertainty in seismic hazard at the four Swiss NPP sites. The main components of the project organization consist of five technical subprojects: (1) seismic source characterization, (2) ground motion characterization, (3) site response characterization, (4) hazard computation and (5) earthquake scenario development.

5. TESTING PROBABILISTIC SEISMIC HAZARD ANALYSIS RESULTS

5.1. INTRODUCTION

Checking the consistency of PSHA results is important given the high uncertainties in SHA and the importance of PSHA results for seismic design. In recent years, increasing efforts have been devoted to assessing the reliability of PSHA results, different kinds of procedures have been tested and many papers have provided useful information on this topic. In 2008, the OECD Nuclear Energy Agency, in cooperation with the IAEA, organized a workshop on Recent Findings and Developments in PSHA: Methodologies and Applications [68]. The main objective was to review recent research and regulatory and industry issues associated with PSHA. Two main recommendations were addressed:

(1) It is very important to undertake consistency checks, which provide valuable information even though a consistency check is a lesser standard than a validation. Guidance on consistency checks should also be a major part of any broader PSHA.

(2) Using Bayesian updating methods can be important and further PSHA work (both research work and applications) in this area is to be encouraged.

The main objective of this section is to give an overview of approaches for testing PSHA and examples of how these tests can be used to adjust PSHA model parameters in order to better reflect what is expected from historical and recent seismic observations. In principle, seismic hazard curves are empirically testable, but in practice, the data required for such tests are difficult to acquire. Which kind of testing procedure is eventually found to be the most appropriate depends on the available data and the objective of the test, in addition to the kinds of tests that are permitted.

In the last decade, several approaches to the testing of PSHA results have been published. Several recent opinion papers encourage hazard analysis to carry out tests (e.g. Refs [69, 70]) and several applications have been made in different countries (France, Italy, New Zealand, USA). The techniques rely on various statistical assumptions. Any testing technique has to address the observation time window that is available. Considering the observation time window in seismology (~100 years maximum for instrumental networks, and several centuries for historical data), testing at the return periods of interest in engineering seismology can be very difficult. PSHA models can be evaluated using different types of observations, such as intensities, 'synthetic' accelerations (converted from intensities or predicted from an earthquake catalogue), true accelerations recorded at instrumented sites or maximum observed acceleration levels based on precarious fragile structures [71–75]. Figure 17 illustrates the observations available for testing different parts of the hazard curve.

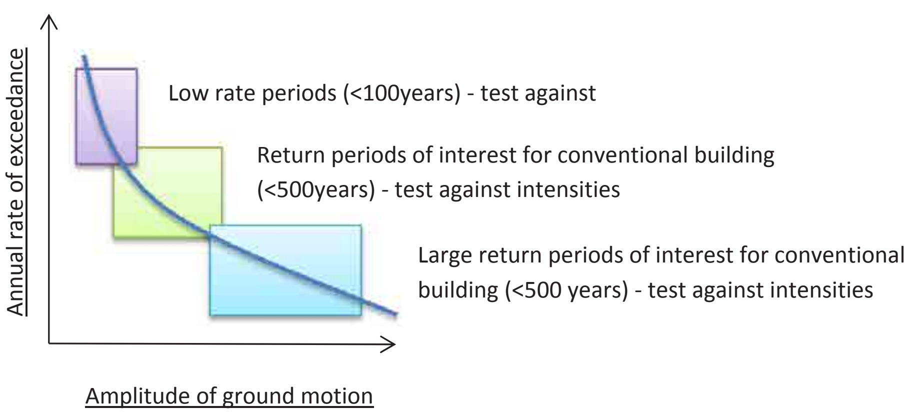

FIG. 17. Diagram illustrating how available observations can be used to constrain different parts of the hazard curves.

5.2. METHOD FOR TESTING PSHA ESTIMATES AGAINST OBSERVATIONS

Ordaz and Reyes [76] published the first study to compare a hazard curve with observed rates of peak accelerations in 1999. It focuses on a single site in Mexico City (the 'Ciudad Universitaria' station), which has been recording continuously since 1962. The empirical hazard curve is built directly from the numbers of the accelerations recorded above various thresholds at the site since the station was installed. The number of observed exceedances is divided by the time interval of observation (35 years), which gives the empirical annual rates of exceedance. These observed rates are superimposed on the hazard curve obtained by applying classical probabilistic methodology, and the fit is evaluated visually (Fig. 18). At first glance, the observations and predictions at the station look rather consistent. However, the observation time window at the site is only 35 years, and for such a short time window, the good fit between predictions and observations might be a coincidence. The limitations due to short observation time windows at individual sites can be reduced by considering several sites (sampling in space). Most techniques proposed to test PSHA estimates rely on this approach, and are introduced below.

In 1995, Ward [77] demonstrated that the length of observation time intervals can be expanded when considering several sites and sampling in

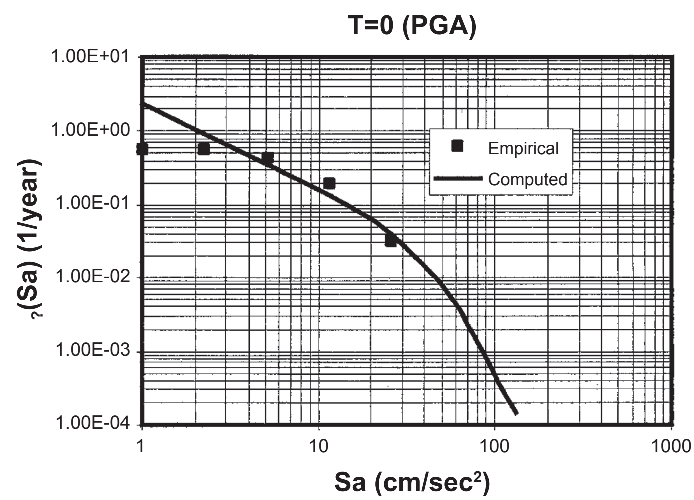

FIG. 18. Observed rates superimposed to the probabilistic seismic hazard curve, for peak ground acceleration, at the Ciudad Universitaria station in Mexico City (reproduced with permission from Ordaz and Reyes [76]).

space. Thus, the consistency of a PSHA model with observations is evaluated, assembling all observed data at several locations.

Stirling and Petersen [78] and Stirling and Gerstenberger [79] proposed a similar approach to that of Ordaz and Reyes [76] using simple statistical techniques to compare the PSHA predictions with observed data and evaluate their consistency with the PSHA estimations. Following the method proposed by these authors, at one site, for a given acceleration threshold (g_0), a PSHA model provides its mean annual rate of exceedance (λ_i). The mean expected number of exceedances is obtained by multiplying the rate times the length of the observation time interval ($\lambda_i t_i$). Accelerations at a site are assumed to occur according to a stationary Poisson process. The Poisson distribution, fully defined by its mean, provides the probability of observing a given number n of accelerations above the threshold g_0:

$$P(n) = \frac{(\lambda_i t_i)^n e^{-\lambda_i t_i}}{n!} \tag{11}$$

where t_i is the time window at site i with an annual rate of exceedance λ_i given by the PSHA model. The authors defined the following simple statistical test: If the observed number falls within the tails of the distribution, defined by the percentiles 2.5 and 97.5, the observations are considered consistent with the model. The sites are far enough apart that they can be considered independent in terms of ground motion exceedances. As the sum of independent Poisson processes constitutes a Poisson process, the total number of exceedances observed over all sites is compared to the distribution defined by the following mean:

$$N_{\text{total}} = \sum_{\text{sites}} \lambda_i t_i \tag{12}$$

In 2009, Fujiwara et al. [80] considered a large set of strong motion sites covering the whole of Japan. The comparison they proposed aims at compensating for short observation time windows by sampling densely in space (~1000 stations). They proposed comparing the probabilistic estimates with the observations in the form of instrumental JMA intensities. They considered the time period from 1997 to 2006. The probabilistic estimate was calculated for the period 1997–2006 (time dependent hazard). They counted how many stations experienced an intensity higher than a given intensity level during that decade, and divided by the total number of stations. Observed ratios of exceedance were obtained for different I_{JMA} levels (5 lower, 5 upper, 6 lower and 6 upper). Then, for a given intensity level, they compared this observed ratio with the mean probability of exceeding the intensity level calculated over all probabilities obtained at the locations of the instrumented sites. K-NET stations experiencing a similar rate of probability of exceedance with a calculated probability of exceedance of intensity (PSHA map) are shown in Table 3. The values are quite close, and the authors conclude that the prediction and the observations are consistent. This study uses a dense network of stations (sampling in space) to compensate for the short time windows of observation at individual sites. The test is the first attempt to use strong motion data to test PSHA estimates in Japan.

TABLE 3. RATIOS OF NUMBER OF STATIONS WITH AT LEAST ONE EXCEEDANCE (OBSERVATIONS) AND AVERAGE PROBABILITY OF EXCEEDING A CERTAIN I_{JMA} LEVEL AS CALCULATED THROUGH THE PROBABILISTIC STUDY
(reproduced with permission from Fujiwara et al. [80])

	Ratio of K-NET stations	PSHA map (all meshes)
≥5 lower	0.232	0.21
≥5 upper	0.099	0.077
≥6 lower	0.029	0.021
≥6 upper	0.006	0.0028

In 2008, Labbé [81] introduced a method that tests a seismic hazard map produced by a PSHA against historical seismicity in the region covered by this map. The method does not consist of directly comparing accelerations with intensities, but of comparing two values of the seismic risk in the region. On the basis of the European Macroseismic Scale (EMS98) [82] the seismic risk is defined as the annual probability that a conventional masonry building experiences damage of at least grade 2 or 3 (according to the EMS98 definitions).

The first risk value is calculated on the basis of the statistical treatment of historical seismicity in France, including more than an hundred isoseismic maps. For this purpose, metropolitan France is divided in territories of approximately homogeneous seismic activity. The second risk value is calculated by the convolution of the hazard map with fragility curves of conventional masonry buildings. These fragility curves were established in the framework of the Risk-UE research project [83].

Three different maps of seismic hazard of France were processed. The author concluded that a first map corresponded to an overestimate of the risk by a factor of 10, a second map to some degree of overestimate, while the third to a slight underestimate. In 2010, Labbé [84] repeated the exercise on the basis of new fragility curves published by Rota et al. [85]. Basically, the conclusions drawn in 2008 were confirmed, although with some slight differences. The method is applicable in any region with well known historical seismicity. It requires that appropriate fragility curves of conventional historical buildings are available.

In 2008, Albarello and D'Amico [86] proposed a method called the counting method which makes use of the binomial distribution, a stochastic process that can result in two outputs: a success or a failure. First, the common longest available time window for the strong motion sites has to be identified. Second, a probability of exceedance is chosen. Albarello and D'Amico selected a 10% probability of exceedance over a 30 year time window (the time life of 68 strong motion stations). Therefore, one value of the probabilistic hazard curve is tested: the acceleration corresponding to 10% probability of exceedance in 30 years. This ground motion level naturally varies depending on the site.

The method relies on the assumption that the occurrences of ground motions at the sites belong to one unique stochastic process. In other words, the occurrences of ground motions larger than a certain threshold during a given time window are realizations of the same stochastic variable. The binomial distribution is a discrete probability distribution that describes the number of successes in a sequence of n experiments (or trials). Each experiment can result either in success (exceedance of the ground motion target g_0) or in failure (the level g_0 was not exceeded during the observation time window). If n stations are considered, then n is the number of trials. Under a binomial distribution, the probability of getting N successes from n trials is:

$$\mathrm{P}(n=N)=\binom{s}{N}p^{N}(1-P)^{s-N} \tag{13}$$

where

$$\binom{s}{N}=\frac{s!}{N!(s-N)!}$$

and where

s is the number of trials;
and p is the probability of success at each trial.

Albarello and D'Amico in 2008 [86] also proposed another approach based on the calculation of likelihoods of observations under the assumption that given models are true. In their application for Italy, 13 out of 68 instrumented sites experienced a ground shaking higher than the predicted threshold (corresponding to 10% probability of being exceeded at least once in 30 years). The likelihood of the observations under the PSHA model can be calculated by the multiplication of the individual probabilities to have experienced a success at 13 sites, and a failure at 55 sites. This calculation can be carried out for different possible PSHA calculations, corresponding to different branches of a logic tree. The model yielding the highest likelihood value is identified as the best fitting PSHA model. This method provides the relative evaluation of different PSHA models instead of evaluating the absolute fit of one PSHA model with the observations.

$$L = \left\{ \prod_{13\,\text{exceedance}} p\left(g \geq g_0\right) \right\} * \left\{ \prod_{55\,\text{no exceedance}} \left(1 - p\left(g \geq g_0\right)\right) \right\} \tag{14}$$

The largest L value implies the best consistency of the PSHA model with the observed data.

5.3. UPDATING METHODS TO IMPROVE ROBUSTNESS OF PSHA

Testing of PSHA is done as a check of whether the results of a PSHA appear to be realistic in comparison to what is expected from known historical and recent seismicity. If the hazard for the tested recurrence interval is much higher or lower than observed data, it suggests that the PSHA model is most likely inappropriate for the selected region. In this case, the test against observed data can be used to calibrate the PSHA model, e.g. by re-evaluating the epistemic uncertainties using Bayesian updating techniques. In recent years, several researchers have proposed an innovative approach that may be used to better address the uncertainties, and allow PSHA to become more robust and consistent with observations [87, 88]. Two examples of the comparison between the initial and updated PSHA prediction models using hazard curves are provided in Figs 19 and 20.

The different approaches discussed in this subsection provide the means to investigate the order of magnitude and robustness of the hazard results. At present, there is no preferred approach or recommendation of which method to use. All of the discussed approaches have limitations and their applicability depends on the information available and on boundary conditions. Nevertheless, the importance of such tests should to be considered to improve the reliability of the PSHA results.

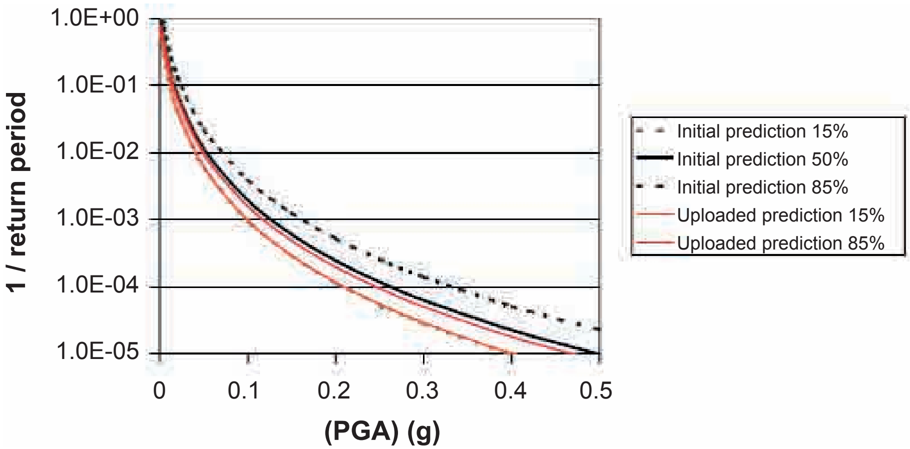

FIG. 19. Hazard curves for initial PSHA model and the updated model using the Bayesian technique (reproduced with permission from Viallet et al. [87]).

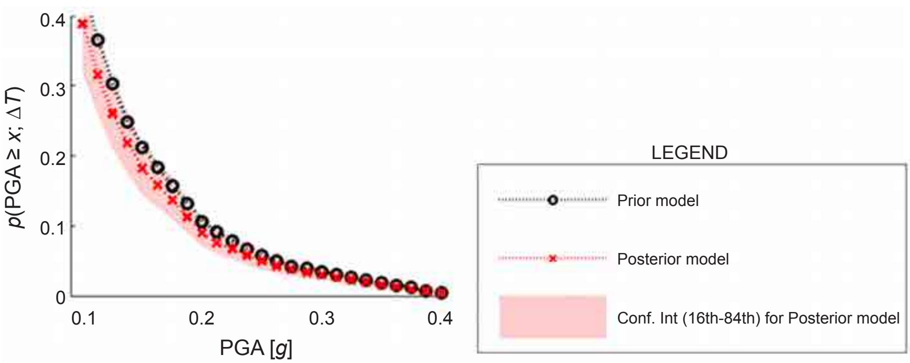

FIG. 20. Hazard curves from prior and posterior PSHA models using observed data through Bayesian inference (reproduced with permission from Selva and Sandri [88]).

6. SUMMARY AND OUTLOOK

In this report, a general guideline is proposed to evaluate seismic hazard caused by diffuse seismicity. The report starts with characterization of diffuse seismicity, and methodologies used in hazard assessment are introduced. Methodologies are carefully selected to match the seismic environment and available information in the target area. Some examples of SHA relating to diffuse seismicity are described in different seismotectonic settings with different methodologies. They may provide useful information to evaluate seismic hazards caused by diffuse seismicity in other target areas.

Aspects of diffuse seismicity are controlled by seismic activity in the target area. In high seismicity areas, the effect of the identified fault is dominant in SHA and the maximum possible magnitude of diffuse seismicity is usually considered to be the lowest limit of identified earthquakes. However, in many stable continental areas, large earthquakes have not been recorded in historical data or palaeoseismological surveys. Therefore, diffuse seismicity is area dependent to some extent. Suitable methodology and parameters should be adopted for each area.

The evaluation of uncertainties for assessing seismic hazard is of great importance. Further studies are encouraged for reducing epistemic uncertainty through a good understanding and modelling of aleatory variability.

As mentioned above, the problems of assessing seismic hazard of diffuse seismicity are as follows:

- How to evaluate seismicity, and source parameters that are suitable for the target area;
- How to reduce uncertainties.

As for the first problem, the difficulty is the limited time span of our knowledge of seismicity. Modern observations began only a hundred years ago. The oldest historical literature is a few thousand years old. This is not long enough to compare the recurrence periods of damaging earthquakes. To cover this weakness, palaeoseismological surveys are expected to provide further information.

To solve the problem of uncertainties, much more observation and exploration are required. Extensive studies are needed to understand the nature of seismic events. Observed records and models of earthquake sources and velocity structures have to be accumulated. Advanced classification between epistemic uncertainty and aleatory variability of parameters might be a breakthrough to reduce uncertainty. Refining methodologies are also required for the purpose.

The evaluation of seismic hazard on diffuse seismicity is a quite ambitious undertaking owing to large uncertainties for individual seismotectonic environments. As recommended in SSG-9 [1], available information has to be considered to as great an extent as possible in the evaluation. Recent international practices and state of the art knowledge have been introduced in this report.

Appendix

PROBABILISTIC SEISMIC HAZARD ANALYSIS USING MONTE CARLO SIMULATION AND FAULT RUPTURE MODELLING FOR SEISMIC HAZARD ANALYSIS IN JAPAN

The content of this appendix has been contributed by JNES.

A.1. INTRODUCTION

Because of the high seismicity in Japan, particular attention is paid to seismic issues in the siting, design and construction of NPPs. For example, in light of the 1995 Kobe earthquake as well as following a decade's accumulation of high quality strong motion observation, the NSC revised the guide in 2006, integrating S1 and S2 into a single level (the DBGM Ss). More detail can be found in Section 4.2.

As introduced in Section 4.2, Kato's spectrum had been used to develop the DBGM Ss without specifying seismic sources. However, JNES proposed a probabilistic approach to address the development of ground motions evaluated without specifying seismic sources [89]. This appendix summarizes the PSHA implemented by JNES, which applies Monte Carlo simulations to generate earthquake occurrences as well source characterization for targeted regions, it evaluates ground motions by using the fault modelling method and assesses seismic hazards such as UHRS.

This appendix summarizes the PSHA implemented by JNES, which applies Monte Carlo simulations to generate earthquake occurrences as well source characterization for targeted regions; evaluates ground motions by using the fault modelling method; and assesses seismic hazards such as UHRS.

A.2. CATEGORIZATION OF INLAND CRUSTAL EARTHQUAKES AND TARGET CATEGORIES

According to the regulatory guides, three types of earthquakes, e.g. inland crustal earthquakes, interplate earthquakes and oceanic intra-plate earthquakes, are required to be taken into account to develop the DBGMs. In contrast to the inland crustal events with a long recurrence period, subduction zone earthquakes in Japan have a relatively short recurrence period and have been instrumentally well observed, enabling the identification of their sources.

In the case of inland crustal earthquakes, there are always some seismic sources that are difficult to identify in advance even when implementing detailed surveys (e.g. geomorphological surveys using aerial photographs or geological field surveys).

A.3. METHODOLOGY OF THE JNES APPROACH

In addition to the development of a probability model of earthquake occurrence with fault traces, this approach features the implementation of Monte Carlo simulations for earthquake location and fault/asperity distribution as well as ground motion simulation by using the fault modelling method.

As shown in Fig. 21, this approach consists of the following four steps: (a) seismicity parameter characterization; (b) Monte Carlo simulations for earthquake generation (including uniform distribution of seismic sources and fault parameters for the sources); (c) strong motion simulation and (d) hazard curve calculation.

A.4. SEISMICITY PARAMETER CHARACTERIZATION

A.4.1. Seismotectonics and regional characteristics in Japan

There are at least three plates in the Japanese archipelago and the surrounding areas: the Pacific Plate, the Philippine Sea Plate, and the continental Eurasian Plate. The Pacific Plate approaches the Japanese archipelago from the east-south-east at a speed of 8 cm annually, whereas the Philippine Sea Plate is approaching the archipelago from the south-east at a speed of roughly 3–7 cm per year; both are subducting under the continental plate. The Japanese archipelago is hence experiencing compression in an east to west direction.

Distinctly, most of the active faults in northern Japan are identified with a reverse sense of slip and run in a north to south direction, whereas those in western Japan usually have a lateral sense of movement and run in a north-east–south-west or north-west–south-east direction (Fig. 22(a)). Focal mechanism solutions show similar characteristics (Fig. 22(b)). Maps of detailed seismotectonic provinces have been proposed based on the information of tectonic geomorphology and geology, characteristics of active faults, seismicity and so on [90]. Those maps, however, are usually too localized to evaluate reliable seismicity parameters. JNES divided the Japanese archipelago into six regions and focused on the North, Kinki, West and Kyushu regions. For example, the seismicity parameters in an area of 314 km^2 for the North region can be characterized as shown in Eq. (15).

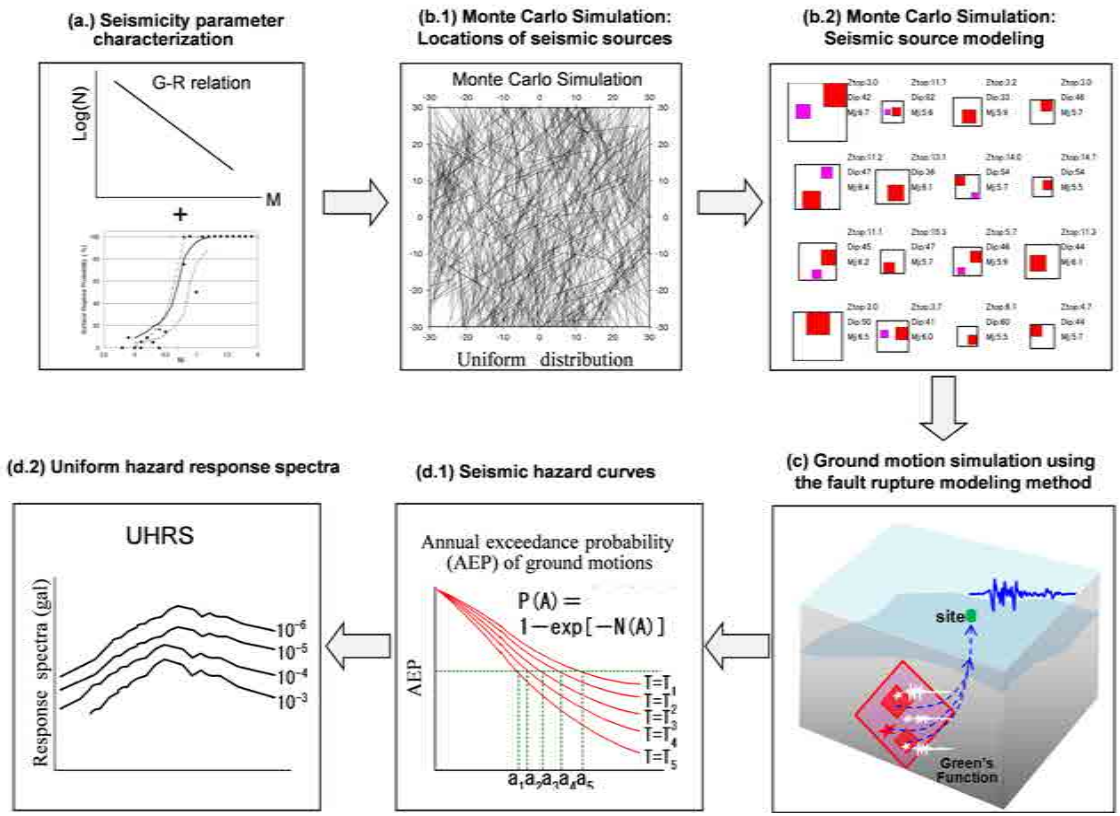

FIG. 21. Flow chart of the JNES approach to formatting ground motions without specifying seismic sources in advance.

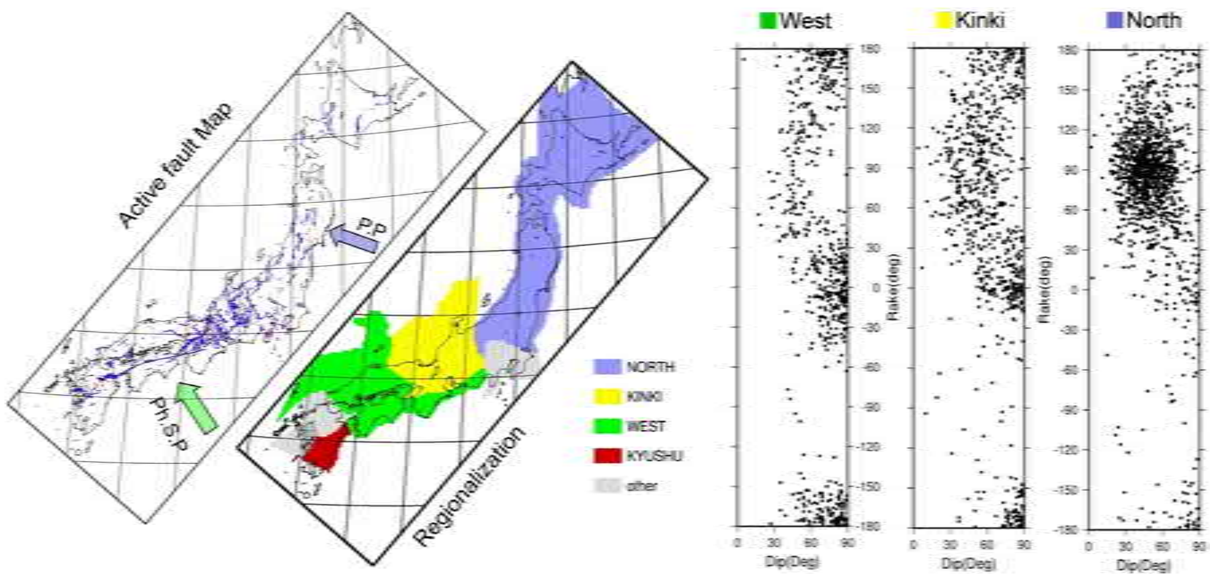

FIG. 22. Division of target areas considering regional characteristics. (a) Regionalization based on the active fault map. (b) Distinct regional characteristics shown by the fault dip and rake distribution from focal mechanism solutions.

$$\log_{10} N(M \geq m) = 2.325 - 0.9846m \tag{15}$$

where N is the number of earthquakes with magnitude larger than m.

A.4.2. Occurrence model for earthquakes with surface rupture

By defining a probability distribution P_{SR} which characterizes the occurrence probability of earthquakes of magnitude m with surface ruptures (SR), JNES constructed the probability model of occurrence for earthquakes of category I and II as follows:

$$P_{\text{Non-SR}}(m) = 1 - P_{SR}(m) \tag{16}$$

In Monte Carlo simulation, this can be realized by defining a certain level of surface deformation as the threshold such that those source models with the calculated maximum surface strain exceeding the threshold value are discarded. Given the source models (which are to be characterized later), the distribution of surface strain can be readily calculated by using theoretical methods (e.g. Ref. [91]). Figure 23 shows that the threshold of the maximum surface

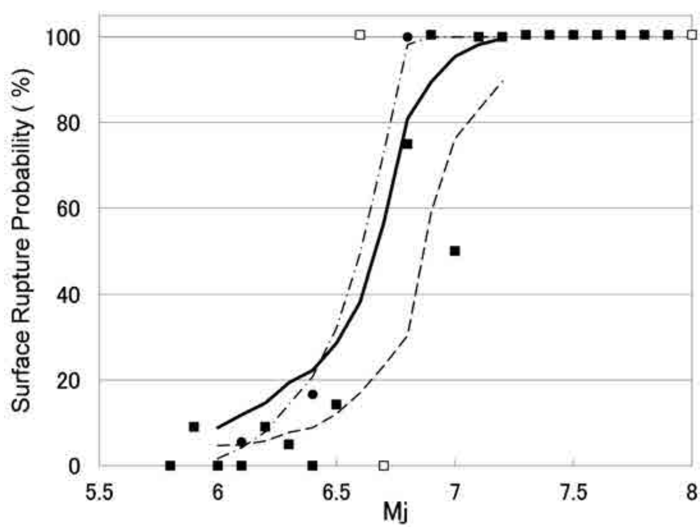

FIG. 23. A probability model (thick black line) for the occurrence of earthquakes with surface rupture (fault traces). The squares indicate the data from field investigations. Two candidate models in terms of the maximum surface strain of 10^{-4} (dashed line) and the surface displacement of 20 cm (dashed dotted line), respectively, are plotted for comparison.

strain 5×10^{-5} fits well the results of previous studies which analysed the surface rupture probability based on observation data (e.g. Refs [92, 93]).

A.5. MONTE CARLO SIMULATIONS

A.5.1. Simulation of spatial distribution

JNES used the Monte Carlo approach to simulate a random distribution of 1000 events for each magnitude in a target area (a total of 25 magnitudes of $5.5 \leq M_j \leq 7.4$ at 0.1 increments). Note that JNES does not apply this approach to generate synthetic catalogues, which are helpful for targeting a wide-region hazard map (e.g. Ref. [94]) but inefficient for a site specific PSHA, since a single catalogue is sufficient to characterize the seismicity parameters in this case. The seismicity rate γ for a certain magnitude m is calculated from the GR relation for a certain magnitude relation (using equation 1 for an area of 314 km^2) as follows:

$$\gamma(m) = (N(M \geq m) - N(M \geq m + 0.1)) \times \frac{S}{314} \tag{17}$$

where S is the area of the target regions.

A.5.2. Source parameter characterization

Following the procedure recommended by the Headquarters for Earthquake Research Promotion [95] in Japan, JNES determined the values of source parameters necessary for the fault modelling method. The source parameters are usually divided into two types: the outer fault parameters, which include the magnitude of the earthquakes and the geometry of the faults, and the inner fault parameters, which consist of the locations and sizes of the asperities (or strong motion generation areas), the stress drops and so on. JNES applied the Monte Carlo approach to simulate the observed pulse-like signals that the asperities / strong motion generation areas tend to concentrate in the centre of the rupture area. Note that the asperity / strong motion generation area location in the depth direction is constrained by the surface strain threshold of 5×10^{-5}. To take into account the uncertainties in the fault parameter determination, the parameters of the dip angle, the location and size of asperities / strong motion generation areas are also allowed to vary in a certain range. Table 4 shows an example of fault parameters determined for an M_j 6.8 earthquake.

TABLE 4. EXAMPLE OF MAIN PARAMETERS USED FOR THIS STUDY

Fault parameters	Estimates			Units
	Small	Average	Large	
Magnitude (Mj)		6.8		
Width of the fault W		26.27		km
Length of the fault L		12.24		km
Rupture area		321.54		km^2
Seismic moment (M_0)		7.25×10^{18}		N·m
Length of asperity I	6.55	7.66	8.63	km
Width of asperity I	4.96	5.81	6.54	km
Area of asperity I	32.49	44.50	56.44	km^2
Seismic moment of asperity I	1.58×10^{18}	2.17×10^{18}	2.75×10^{25}	N·m
Slip value of asperity I	147.1	147.1	147.1	cm
Length of asperity II	4.18	4.89	4.89	km
Width of asperity II	4.18	4.89	5.51	km
Area of asperity II	17.47	23.91	30.36	km^2
Seismic moment of asperity II	6.26×10^{17}	8.56×10^{17}	1.09×10^{17}	N·m
Slip value of asperity II	108	108	108	cm
Stress drop of asperities	19.676	14.38	11.331	MPa
Size of the background area	271.58	253.13	234.74	km^2
Moment of the background area	5.04×10^{18}	4.22×10^{18}	3.41×10^{18}	N·m
Slip value of background area	56	50.4	43.9	cm
Stress drop of the background area	2.593	2.065	1.658	MPa

A.6. Ground motion simulation

The DBGM is determined at the free ground surface of an outcrop or a hypothetical outcrop, which is referenced to the in situ layer specified by a shear wave velocity of no less than 700 m/s according to Japanese regulatory guides [57]. To take account of site response for ground motion simulations, construction of a site specific underground structure model characterizing parameters of the ground velocity structure between the reference layer and the seismic bedrock is needed. As Table 5 shows, the model is usually horizontally layered using the thickness, density, seismic wave velocities and Q values of each layer. Using the characterized source models established above, ground motions were simulated using the revised stochastic Green's function method [96]. Figure 24 shows the calculated response spectra with 5% damping from the simulations conducted for the M_j 6.8 earthquakes (a total of 1000 events). The variation of simulated ground motions is larger in the longer period range. This occurs because the fault rupture propagation effect is larger at long periods than at short periods, and the larger the earthquake, the longer the period of the ground motions that are affected.

TABLE 5. UNDERGROUND STRUCTURE MODEL FOR THE KINKI REGION

Depth to top (m)	Thickness (m)	Density (kg/m^3)	V_p (m/s)	V_s (m/s)	Q_s
10	34	2.6	3700	1450	16.7
44	86	2.6	4300	1760	16.7
130	500	2.6	4600	2200	16.7
630	770	2.6	5130	2800	50.0
1400	2800	2.6	5310	3100	50.0
4000	—	2.7	6270	3600	50.0

By counting the number of calculated spectra that exceed a value of y at a period of T, the following formula was used to estimate the probability of exceedance of ground motion y for an $M_j = m$ event which is not a Category III earthquake:

$$\mathrm{P}\left(\mathrm{Y}(T) \geq \mathrm{y}|m\right) = \frac{N\left(Y \geq y \mid m\right)}{N_{\text{total}}(m)} \tag{18}$$

where N_{total} (m) is the total number of events simulated for a specific magnitude m.

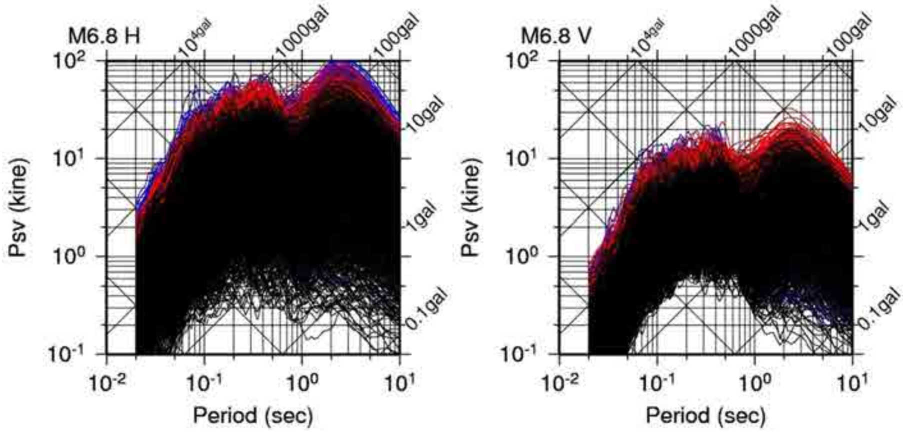

FIG. 24. Examples of simulated ground motions calculated as (a) horizontal and (b) vertical response spectra. Colour spectra are ground motions within a very short distance (images courtesy of the Japan Nuclear Energy Safety Organization).

A.7. Seismic hazard assessment

By assuming a Poisson model, the annual probability P $(Y \geq y)$ of exceedance of a specific ground motion y is given by:

$$P\left(Y \geq y\right) = 1 - \exp\left(-\upsilon\left(Y \geq y\right)\right) \tag{19}$$

where $\upsilon(Y \geq y)$ is the annual frequency of exceedance of the specific level y and can be calculated as follows:

$$\upsilon\left(Y \geq y\right) = \sum_{i}\left(1 - P_{\text{SR}}\left(m_i\right)\right)\gamma\left(m_i\right)P(Y \geq y \mid m_i) \tag{20}$$

for magnitude m_i (ranges from $5.5 \leq M_{\text{j}} \leq 7.4$ at 0.1 increments).

Figure 25 shows the comparison of the hazard curves of the annual probability of exceedance in two periods for the four regions. Figure 26 plots the UHRS at annual exceedance probabilities of 10^{-3}, 10^{-4}, 10^{-5} and 10^{-6}.

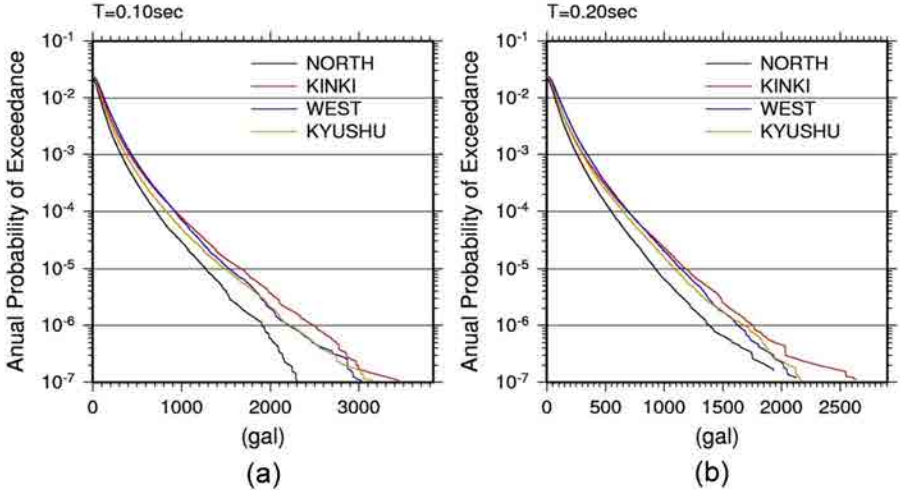

FIG. 25. Comparison of seismic hazard curves. (a) Hazard curves for ground motions of the period of 0.1 second; (b) Hazard curves for ground motions of the period of 0.2 second (images courtesy of the Japan Nuclear Energy Safety Organization).

A.8. Discussion

The above results are comparable with those of a previous study implemented by JNES [60]. The previous study applied the fault modelling method to simulate the ground motions generated at many evaluation points by considering 40 scenario earthquakes and assuming that the distribution of many blind faults around the evaluation point is equivalent to the distribution of many evaluation points around the fault. This assumption holds well for the effects of rupture directivity. However, the Monte Carlo approach not only works well at treating the effects of rupture directivity but is also able to take account of the variability of the fault parameters, such as the location and the size of the asperity.

Japanese utilities have been using the Kato spectrum to develop the DBGM Ss to meet the requirement of considering ground motion evaluated without specifying seismic sources. These probabilistic results show that the Kato spectrum at short periods is between the UHRS of the annual exceedance probability of 10^{-4} and 10^{-5}. It is believed that such a level of DBGM is sufficient to ensure that the core damage frequency will not exceed 10^{-5} / reactor-year. Moreover, given that a safety goal of core damage frequency is defined, the DBGM could be reversely developed using the probabilistic method.

This method can be applied to any region as long as the underground structure at the site is well investigated and the seismicity parameters in the

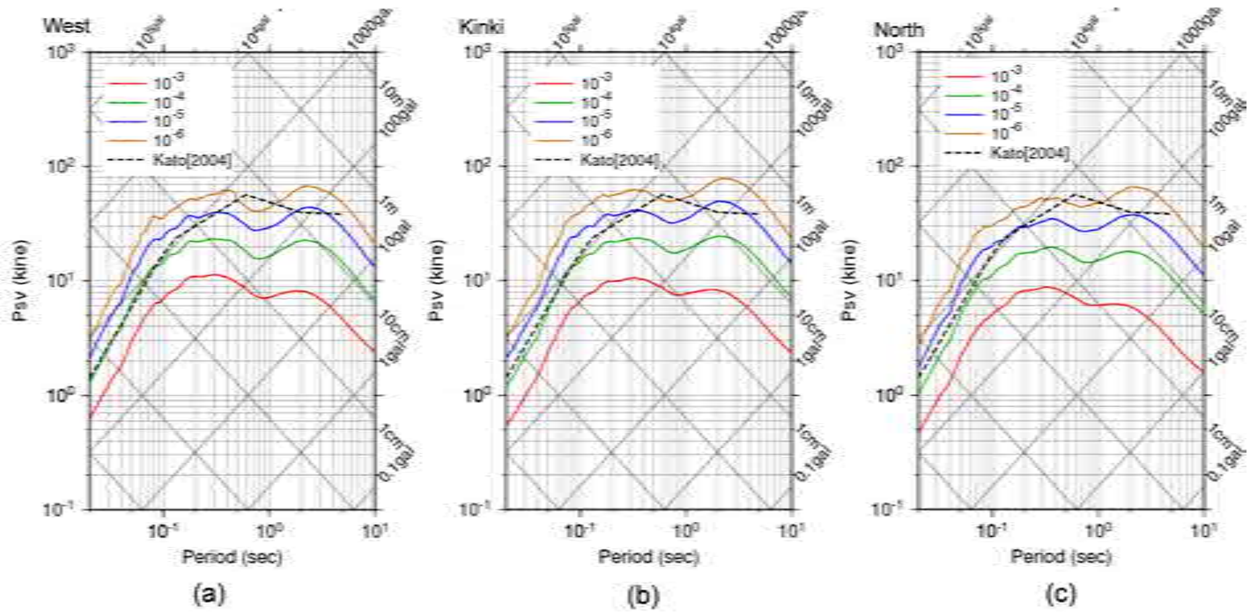

FIG. 26 Region specific UHRS. The results for the North, Kinki and West regions are plotted from right to left. The dashed line indicates the Kato spectrum (courtesy of the Japan Nuclear Energy Safety Organization).

target region are well defined. Without sufficient data, reliable estimation of the seismicity parameters is usually difficult in low seismicity areas. This difficult situation could be improved in the future as more progress is made in instrumental observation as well as in historical and/or palaeoseismological surveys. An alternative is to include the seismicity data of neighbouring regions that are assumed to be under similar seismotectonic conditions. The Flinn-Engdahl regionalization scheme [97] is such an example.

A.9 Conclusions

To address the development of DBGM using ground motions evaluated without specifying seismic sources, a probabilistic method combining the Monte Carlo simulation with the ground motion simulation method was proposed. The determination of the occurrence of the target earthquakes and the characterization of the seismic sources are realized using the Monte Carlo approach. Ground motions are then evaluated by applying the fault modelling method. Seismic hazards, including the annual exceedance probability curves and the UHRS, are calculated by statistically analysing the estimates of ground motions.

REFERENCES

[1] INTERNATIONAL ATOMIC ENERGY AGENCY, Seismic Hazards in Site Evaluation for Nuclear Installations, IAEA Safety Standards Series No. SSG-9, IAEA, Vienna (2010).

[2] SCHWARTZ, D.P., COPPERSMITH, K.J., Fault behavior and characteristic earthquakes: examples from the Wasatch and San Andreas fault zones, J. Geophys. Res. **89** B7 (1984) 5681–5698.

[3] WESNOUSKY, S.G., SCHOLZ, C.H., SHIMAZAKI, K., MATSUDA, T., Earthquake frequency distribution and the mechanics of faulting, J. Geophys. Res. **88** B11 (1983) 9331–9340.

[4] INTERNATIONAL ATOMIC ENERGY AGENCY, Ground Motion Simulation Based on Fault Rupture Modelling for Seismic Hazard Assessment in Site Evaluation for Nuclear Installations, Safety Reports Series No. 85, IAEA, Vienna (2015).

[5] HEADQUARTERS FOR EARTHQUAKE RESEARCH PROMOTION, Seismic Activity in Japan (1999),
http://www.hp1039.jishin.go.jp/eqchreng/eqchrfrm.htm

[6] INTERNATIONAL ATOMIC ENERGY AGENCY, The Contribution of Palaeoseismology to Seismic Hazard Assessment in Site Evaluation for Nuclear Installations, IAEA-TECDOC-1767, IAEA , Vienna (2015).

[7] SHIMAZAKI, K., "Small and large earthquakes: The effect of the thickness of seismogenic layer and the free surface", Earthquake Source Mechanics, American Geophysical Union Geophysical Monograph, Vol. 37, AGU, Washington, DC (1986) 209–216.

[8] STUCCHI, M., et al., The SHARE European Earthquake Catalogue (SHEEC) 1000–1899, J. Seismol. **17** 2 (2012) 523–544.

[9] GRÜNTHAL, G., WAHLSTRÖM, R., The European-Mediterranean Earthquake Catalogue (EMEC) for the last millennium, J. Seismol. **16** 3 (2012) 535–570.

[10] GRÜNTHAL, G., WAHLSTRÖM, R., STROMEYER, D, The SHARE European Earthquake Catalogue (SHEEC) for the time period 1900–2006 and its comparison to the European-Mediterranean Earthquake Catalogue (EMEC), J. Seismol. **17** 4 (2013) 1339–1344.

[11] KANAMORI, H., The energy release in great earthquakes, J. Geophys. Res. **82** 20 (1977) 2981–2876.

[12] INTERNATIONAL ASSOCIATION OF SEISMOLOGY AND PHYSICS OF THE EARTH'S INTERIOR, Summary of Magnitude Working Group Recommendations on Standard Procedures for Determining Earthquake Magnitudes from Digital Data (2005), http://www.iaspei.org/commissions/CSOI.php

[13] HEATON, T.H., TAJIMA, F., MORI, A.W., Estimating ground motions using recorded accelerograms, Surv. Geophys. **8** (1986) 25–83.

[14] GARDNER, J.K. KNOPOFF, L., Is the sequence of earthquakes in Southern California, with aftershocks removed, Poissonian? Bull. Seismol. Soc. Am. **64** 4 (1974) 1363–1367.

[15] REASENBERG, P., Second-order moment of central California seismicity, J. Geophys. Res. **90** (1985) 1969–1982.

[16] TINTI, S. MULARGIA, F., Completeness analysis of a seismic catalog, Ann. Geophys. **3** (1985) 407–414.

[17] ALBARELLO, D., CAMASSI, R., REBEZ, A., Detection of space and time heterogeneity in the completeness level of a seismic catalogue by a “robust” statistical approach: an application to the Italian area, Bull. Seismol. Soc. Am. **91** 6 (2001) 1694–1703.

[18] STEPP, J.C., An Investigation of Earthquake Risk in the Puget Sound Area by Use of the Type I Distribution of Largest Extremes, PhD Thesis, Pennsylvania State Univ. (1971).

[19] STEPP, J.C., “Analysis of completeness of the earthquake sample in the Puget Sound area and its effect on statistical estimates of earthquake hazard”, Proc. 2nd Int. Conf. on Microzonation for Safer Construction Research and Application, San Francisco, CA, 1978, United States National Science Foundation, Arlington, VA (1978) 897–909.

[20] CORNELL, C.A.. Engineering seismic risk analysis, Bull. Seism. Soc. Am. **58** (1968) 1583–1606.

[21] RICHTER, C.F., Elementary Seismology, W.H. Freeman, San Francisco, CA (1958).

[22] GUTENBERG, B. RICHTER, C.F., Frequency of earthquakes in California, Bull. Seismol. Soc. Am. **34** 4 (1944) 185–188.

[23] AKI, K., Maximum likelihood estimate of b in the formula log N = a - bM and its confidence limits, Bull. Earthq. Res. Inst. **43** (1965) 237–239.

[24] MOLCHAN, G.M., KEILIS-BOROK, V.I., VILKOVICH, G.V., Seismicity and principal seismic effects, Geophys. J. **21** (1970) 323–335.

[25] WEICHERT, D.H., Estimation of the earthquake recurrence parameters for unequal observation periods for different magnitudes, Bull. Seismol. Soc. Am. **70** 4 (1980) 1337–1346.

[26] KIJKO, A. SMIT, A., Extension of the b-value estimator for incomplete catalogs, Bull. Seismol. Soc. Am. **102** 3 (2012) 1283–1287.

[27] FRANKEL, A., Mapping seismic hazard in the Central United States, Seismol. Res. Lett. **66** 4 (1995) 8–21.

[28] FIX, E., HODGES, J.L., Discriminatory Analysis, Nonparametric Estimation: Consistency properties, Technical Report,. Report No. 4, Project No. 21-49-004, United States Air Force School of Aviation Medicine, Randolph Field, TX (1951).

[29] SILVERMAN, B.W., Density Estimation for Statistics and Data Analysis, Monographs on Statistics and Applied Probability Vol. 26, Chapman and Hall, London (1986).

[30] BENDER, B., Modeling source zone boundary uncertainty in seismic hazard analysis, Bull. Seismol. Soc. Am. **76** 2 (1986) 329–341.

[31] VENECIANO, D., PAIS, A.L., “Automatic source identification based on historical seismicity”, Proc. 8th European Conf. on Earthquake Engineering, Lisbon, 1986, Laboratório Nacional de Engenharia Civil, Lisbon (1986).

[32] ELECTRIC POWER RESEARCH INSTITUTE Seismic Hazard Methodology for the Central and Eastern United States, Series No. NP-4726, 10 Vols, EPRI, Palo Alto, CA (1986).

[33] NUCLEAR REGULATORY COMMISSION, DEPARTMENT OF ENERGY, ELECTRIC POWER RESEARCH INSTITUTE, Central and Eastern United States –

Seismic Source Characterization for Nuclear Facilities, Rep. NUREG-2115, EPRI, Palo Alto, CA (2012).
[34] PELÁEZ-MONTILLA, J.A., LÓPEZ-CASADO, C., Seismic hazard estimate at the Iberian peninsula, Pure and Appl. Geophys. **159** (2002) 2699–2713.
[35] JAISWAL, K., SINHA, R., Probabilistic modeling of earthquake hazard in stable continental shield of the Indian peninsula, ISET J. Earthq. Technol. **43** 3 (2006) 49–64.
[36] BOMMER, J.J., STAFFORD, P.J., ALARCÓN, J.E., AKKAR, S., The influence of magnitude range on empirical ground motion prediction, Bull. Seismol. Soc. Am. **97** (2007) 2152–2170.
[37] ABRAHAMSON, N.A., SILVA, W.J., KAMAI, R., Update of the AS08 Ground-motion Prediction Equations Based on the NGA-West2 Data Set, PEER Report No. 2013/04, Pacific Earthquake Engineering Research Center, Berkeley, CA (2013).
[38] JOHNSTON, A. C., KANTER, L. R., Earthquakes in stable continental crust, Scientific American (1 Mar. 1990) 68–75.
[39] KIJKO, A., Estimation of the maximum earthquake magnitude, Mmax, Pure and Appl. Geophys. **161** (2004) 1–27.
[40] DOUGLAS, J., Ground-Motion Prediction Equations 1964–2010, PEER Report 2011/102, Pacific Earthquake Engineering Research Center, Berkeley, CA (2011).
[41] STEWART J.P, et al., Implications of Mw 9.0 Tohoku-oki Japan earthquake for ground motion scaling with source, path, and site parameters, Earthq. Spectra **29** Suppl. 1 (2013) S1–S21.
[42] SOMERVILLE, P.G., SMITH, N.F., GRAVES, R.W., ABRAHAMSON, N.A., Modification of empirical strong ground motion attenuation relations to include the amplitude and duration effects of rupture directivity, Seismol. Res. Lett. **68** (1997) 199–222.
[43] SOMERVILLE, P.G., et al., Characterizing crustal earthquake slip models for the prediction of strong ground motion, Seismol. Res. Lett. **70** (1999) 59–80.
[44] NATIONAL RESEARCH INSTITUTE FOR EARTH SCIENCE AND DISASTER PREVENTION, Strong-motion Seismograph Networks (K-NET, KIK-net) (2004), www.kyoshin.bosai.go.jp/kyoshin/quake
[45] CAMPBELL K. W., Empirical near-source attenuation relationships for horizontal and vertical components of peak ground acceleration, peak ground velocity, and pseudo-absolute acceleration response spectra, Seismol. Res. Lett. **68** (1997) 154–179.
[46] KATO, K., et al., Earthquake ground motions by blind faults in the upper crust: Categorization of earthquakes based on geological survey and examination of the upper level from strong motion records, J. Japan Assoc. for Earthq. Eng. **4** (2004) 46–86 (in Japanese with English abstract).
[47] NISHIMURA, I., et al., “Response spectra for design purpose of stiff structures on rock sites”, Trans. 16th Inter. Conf. Structural Mechanics in Reactor Technology (SMiRT 16), Div.K, No.1133, International Association for Structural Mechanics in Reactor Technology, Raleigh, NC (2001).
[48] GRAVES, R., et al., CyberShake, A physics-based seismic hazard model for Southern California, Pure and Appl. Geophys. **168** 3/4 (2010) 367–381.
[49] ATKINSON, G.M., Single-station sigma, Bull. Seismol. Soc. Am. **96** 2 (2006) 446–455.

[50] RODRIGUEZ-MAREK, A., MONTALVA, G., COTTON, F., BONILLA, F., Analysis of single-station standard deviation using the KiK-net data, Bull. Seismol. Soc. Am. **101** (2011) 1242–1258.
[51] RODRIGUEZ-MAREK, A., et al., A model for single-station standard deviation using data from various tectonic regions, Bull. Seismol. Soc. Am. **103** 6 (2013) 3149–3163.
[52] ABRAHAMSON, N.A., HOLLENBACK, J.C., Application of Single-Station Sigma Ground Motion Prediction Equations in Practice, Proceedings of the 15th World Conference on Earthquake Engineering, Lisbon, Portugal (2012),
[53] TORO, G.R., ABRAHAMSON, N.A., SCHNEIDER, J.F., Modeling of strong ground motions from earthquakes in Central and Eastern North America: Best estimates and uncertainties, Seismol. Res. Lett. **68** (1997) 41–57.
[54] ABRAHAMSON, N.A., SOMERVILLE, P.G., CORNELL, C.A., "Uncertainty in numerical strong motion predictions", Proc. 4th U.S. Nat. Conf. on Earthquake Engineering, Palm Springs, CA, 1990, Vol. 1, Earthquake Engineering Research Institute, El Cerrito, CA (1990) 407–416.
[55] COTTON, F., ARCHULETA, R., CAUSSE, M., What is sigma of the stress drop? Seismol. Res. Lett. **84** 1 (2013) 42–48.
[56] ATOMIC ENERGY COMMISSION, Hatsudenyou Genshiroshisetsunikansuru Taishinsekkeishinsashishin, AEC, Tokyo (1978) (in Japanese).
[57] JAPANESE NUCLEAR SAFETY COMMISSION, Regulatory Guide for Reviewing Seismic Design of Nuclear Power Reactor Facilities, NSC, Tokyo (2006).
[58] NUCLEAR REGULATION AUTHORITY, Outline of New Regulatory Requirements for Light Water Nuclear Power Plants (Earthquakes and Tsunamis) (2013), http://www.nsr.go.jp/data/000067118.pdf
[59] MOTOHASHI, S., et al., Probabilistic evaluation of near-field ground motions due to buried-rupture earthquake caused by undefined faults, Trans. 18th Inter. Conf. Structural Mechanics in Reactor Technology (SMiRT 18), No. KM01-3, International Association for Structural Mechanics in Reactor Technology, Raleigh, NC (2005).
[60] MOTOHASHI, S., EBISAWA, K., SAKAGAMI, M., "Probabilistic evaluation of near-field ground motions due to buried-rupture earthquakes caused by undefined faults", Proc. Specialist Meeting on the Seismic Probabilistic Safety Assessment of Nuclear Facilities, Jeju Island, Republic of Korea, OECD Publishing, Paris (2007) 196–208.
[61] NUCLEAR SAFETY AUTHORITY, Determination of the Seismic Risk for the Safety of Surface Basic Nuclear Installations (2001), http://www.french-nuclear-safety.fr/References/Safety-Rules/Basic-safety-rule-2001-01-of-31-may-2001
[62] BERGE-THIERRY, C., GRIOT-POMMERA, D., COTTON, F., FUKUSHIMA, Y., New empirical response spectral attenuation laws for moderate European earthquakes, J. Earthq. Eng. **7** 2 (2003) 193–222.
[63] BAUMONT D., RUIZ, J., BERGE-THIERRY, C., CUSHING, M., On the Simulations of Broadband Strong Ground Motions for Moderate Earthquakes along the Durance Fault (2004), http://www.oecd-nea.org/nsd/workshops/SEIS2004/Papers/Papers/FR_baumont_s1.pdf

[64] NUCLEAR SAFETY STANDARDS COMMISSION, Design of Nuclear Power Plants against Seismic Events, Part 1: Principles (2011), http://www.kta-gs.de/e/standards/2200/2201_1_engl_2011_11.pdf
[65] SWISS FEDERAL NUCLEAR SAFETY INSPECTORATE, Probabilistic Safety Analysis (PSA): Quality and Scope (2009), http://static.ensi.ch/1314020685/a005_e.pdf
[66] NATIONALE GENOSSENSCHAFT FÜR DIE LAGERUNG RADIOAKTIVER ABFÄLLE, Probabilistic Seismic Hazards Analysis for Swiss Nuclear Power Plant Sites (PEGASOS Project), Final Report, 6 Vols, NAGRA, Wettingen, Switzerland (2004).
[67] SWISSNUCLEAR, Probabilistic Seismic Hazards Analysis for Swiss Nuclear Power Plant Sites (PEGASOS Refinement Project), Final Report, 6 Vols, Swissnuclear, Olten, Switzerland (2013).
[68] Recent Findings and Developments in Probabilistic Seismic Hazards Analysis (PSHA) Methodologies, (Proc. OECD/NEA Workshop, Lyon, France, 2008) OECD Publishing, Paris (2008).
[69] STEIN, S., Bad assumptions or bad luck: Why earthquake hazard maps need objective testing, Seismol. Res. Lett. **82** 5 (2011).
[70] STIRLING, M.W., Earthquake hazard maps and objective testing: The hazard mapper's point of view, Seismol. Res. Lett. **83** 2 (2012).
[71] BRUNE, J.N., Precarious-rock constraints on ground motion from historic and recent earthquakes in Southern California, Bull. Seismol. Soc. Am. **92** 7 (2002) 2602–2611.
[72] BEAUVAL, C., BARD, P.-Y., HAINZL, S., GUÉGUEN, P., Can strong-motion observations be used to constrain probabilistic seismic-hazard estimates? Bull. Seismol. Soc. Am. **98** (2008) 509–520.
[73] BEAUVAL, C., "On the use of observations for constraining probabilistic seismic hazard estimates - brief review of existing methods", paper presented at Int. Conf. on Applications of Statistics and Probability in Civil Engineering, Zurich, 2011.
[74] ANDERSON, J.G., BRUNE, J.N., BIASI, G., ANOOSHEHPOOR, A., PURVANCE, M., Workshop report: Applications of precarious rocks and related fragile geological features to U.S. National Hazard Maps, Seismol. Res. Lett. **82** (2011) 431–441.
[75] BAKER, J., ABRAHAMSON, N., WHITNEY, J.W., BOARD, M.P., HANKS, T., Use of fragile geologic structures as indicators of unexceeded ground motions and direct constraints on probabilistic seismic hazard analysis, Bull. Seismol. Soc. Am. **103** (2013) 1898–1911.
[76] ORDAZ, M., REYES, C., Earthquake hazard in Mexico City: Observations versus computations, Bull. Seismol. Soc. Am. **89** (1999) 1379–1383.
[77] WARD, S., A multidisciplinary approach to seismic hazard in Southern California, Seismol. Res. Lett. **84** (1995) 1293–1309.
[78] STIRLING, M.W., PETERSEN, M.D., Comparison of the historical record of earthquake hazard with seismic hazard models for New Zealand and the continental United States, Bull. Seismol. Soc. Am. **96** (2006) 1978–1994.
[79] STIRLING, M.W., GERSTENBERGER, M.C., Ground motion-based testing of seismic hazard models in New Zealand, Bull. Seismol. Soc. Am. **100** 4 (2010) 1407–1414.

[80] FUJIWARA, H., et al., Statistical comparison of National Probabilistic Seismic Hazard Maps and frequency of recorded JMA seismic intensities from the K-NET strong-motion observation network in Japan during 1997-2006, Seismol. Res. Lett. 80 3 (2009) 458–464.
[81] LABBÉ, P., “Comparison of two methods of seismic assessment in France”, Paper presented at 14th World Conf. on Earthquake Engineering, Beijing, 2008.
[82] EUROPEAN SEISMOLOGICAL COMMISSION, European Macroseismic Scale 1998, EMS-98 (Grünthal, G., Ed.), Cahiers du Centre Européen de Géodynamique et de Séismologie 15, Centre Européen de Géodynamique et de Séismologie, Luxembourg (1998) 99 pp.
[83] MOUROUX, P., LE BRUN, B., “Risk-Ue project, An advanced approach to earthquake risk scenarios with applications to different European towns”, Assessing and Managing Earthquake Risk, Geotechnical, Geological and Earthquake Engineering No. 2, Springer, Dordrecht, Netherlands (2006).
[84] LABBÉ, P., “PSHA outputs versus historical seismicity, example of France”, paper presented at 14th European Conf. of Earthquake Engineering, Ohrid, The Former Yugoslav Republic of Macedonia, 2010.
[85] ROTA, M., PENNA, A., MAGENES, G., A methodology for deriving analytical fragility curves for masonry buildings based on stochastic nonlinear analyses, J. Eng. Struct. **32** (2010) 1312–1323.
[86] ALBARELLO, D., D’AMICO, V., Testing probabilistic seismic hazard estimates by comparison with observations; an example in Italy, Geophys. J. Int. 175 3 (2008) 1088–1094.
[87] VIALLET, E., HUMBERT, N., MARTIN, C., SECANELL, R., “On the use of a Bayesian updating technique to get probabilistic seismic hazard assessment more rugged”, Paper presented at 14th World Conf. on Earthquake Engineering, Beijing, 2008.
[88] SELVA, J., SANDRI, L., Probabilistic seismic hazard assessment: Combining Cornell-like approaches and data at sites through Bayesian inference, Bull. Seismol. Soc. Am. **103** 3 (2013) 1709–1722.
[89] JAPAN NUCLEAR ENERGY SAFETY ORGANIZATION, On Development and Improvement for Evaluation of exceedance probability of design basis ground motion (2012),
www.nsr.go.jp/archive/jnes/content/000123375.pdf
[90] KAKIMI, T., MATSUDA, T.I., AIDA, KINUGASA, Y., A seismotectonic province map in and around the Japanese islands, Zisin 55 (2003) 3893 (in Japanese with English abstract).
[91] OKADA, Y., Internal deformation due to shear and tensile faults in a half-space, Bull. Seismol. Soc. Am. **82** (1992) 1018–1040.
[92] TAKEMURA, M., Scaling law for Japanese intraplate earthquakes in special relations to the surface faults and damages, Zisin **51** (1998) 211–228 (in Japanese).
[93] KAGAWA, T., DAN, K., OHTSUKA, Y., MOTOHASHI, S., A technique setting probability of buried rupture earthquake for probabilistic earthquake hazard estimation, J. Earthq. Eng. 28 (2005) 100 (in Japanese with English abstract).

[94] TAVAKOLI, B., MONTERROSO, D., Monte Carlo seismic hazard maps for northern Central America, covering El Salvador and surrounding area, Geol. Soc. Am. **375** (2004).

[95] HEADQUARTERS FOR EARTHQUAKE RESEARCH PROMOTION, Strong Ground Motion Prediction Method (on RS FOR EARTEarthquakes with Specified Source Faults (2008),
http://www.jishin.go.jp/main/kyoshindo/08apr_kego/recipe.pdf, (in Japanese).

[96] KAGAWA, T., Developing a stochastic Green's Function method having more accuracy in long period range to be used in the Hybrid Method, J. Japan Assoc. for Earthq. Eng. **4** 2 (2004) (in Japanese with English Abstract).

[97] YOUNG, J. B., PRESGRAVE, B.W., AICHELE, H., WIENS, D.A., FLINN, E.A., The Flinn-Engdahl regionalisation scheme: The 1995 revision, Phys. of the Earth and Planet. Inter. **96** 4 (1996) 223−297.

Annex

EXAMPLES OF AVAILABLE DATA

The appendix presents examples of data for seismic hazard analyses that was publicly available as of the end of 2015.

A–1. SEISMIC CATALOGUE

The following sources provide useful information for compiling a seismic catalogue.

- International Seismological Center (ISC)Instrumental catalogue: Year 1900 to present, location and M_W.
  Global historical earthquake catalogue: Year 1000–1903, M_W > 7.0, 800 earthquakes.
- Harvard earthquake catalogue: Year 1976 to present.
- USGS (United States Geological Survey)
  ANSS comprehensive catalog: Year 1973 to present (issued monthly)
  Centennial catalogue: Year 1900–2008, M < 5.5 (1964 to present), M < 6.5 (1930 to present), M <7.0 (1900–).
- JMA (Japan Meteorological Agency)
  Instrument catalogue: Year 1923 to present, M > 2.0, location and M_J.
  Utsu catalogue for Japanese earthquakes: Year 1885–1925, M > 6.
  Usami catalogue for Japanese earthquakes: Year 416 to present, M < 5 (1900 to present), M < 6 (1600 to present), M < 7 (700 to present).

A–2. SEISMIC SOURCE MODEL

If the catalogues are not sufficient, local micro seismicity catalogues will be required. Such information requires a dense high sensitivity and broadband observation network such as:

- High-NET, National Research Institute for Earth Science and Disaster Prevention (NIED), Japan;
- Norwegian Seismic Array (NORSAR).

If geometrical parameters of source rupture are required for constructing seismic source models, moment tensor database are available from the following organizations.

— The Global Centroid Moment Tensor (CMT) Project
— Incorporated Research Institute for Seismology (IRIS)
— USGS, USA
— JMA, Japan
— F-NET, NIED, Japan

When setting source parameters referring to past large earthquakes, the following source rupture databases are useful:

— Pacific Earthquake Engineering Research Center (PEER);
— Finite-source rupture model database (SRCMOD);
— Seismo Note, Nagoya University (NGY), Japan (year 2007 to present);
— Earthquake Information Center (EIC) Seismological Notes, Earthquake Research Institute (ERI), University of Tokyo, Japan (year 1996–2007).

LIST OF ABBREVIATIONS

ANSS	Advanced National Seismic System
CEUS	Central and Eastern United States Seismic Source Characterization
DBGM	design basis ground motion
GMPE	ground motion prediction equation
GR	Gutenberg-Richter relation
HERP	Headquarters for Earthquake Research Promotion
ISC	International Seismological Centre
JMA	Japan Meteorological Agency
JNES	Japan Nuclear Energy Safety organization
NPP	nuclear power plant
PSA	probabilistic safety assessment
PSHA	probabilistic seismic hazard analysis
RLME	repeated large magnitude earthquake
SHA	seismic hazard assessment
UHRS	uniform hazard response spectra

CONTRIBUTORS TO DRAFTING AND REVIEW

Albarello, D.	University of Siena, Italy
Anderson, J.	University of Nevada, United States of America
Berge-Thierry, C.	Alternative Energies and Atomic Energy Commission, France
Crespo, M.J.	PRINCIPIA, Spain
Ebisawa, K.	Central Research Institute of Electric Power Industry, Japan
Fukushima, Y.	International Atomic Energy Agency
Gülen, L.	Sakarya University, Turkey
Irikura, K.	Aichi Institute of Technology, Japan
Kagawa, T.	Tottori University, Japan
Labbé, P.	Électricité de France, France
Martin, C.	Geoter-FUGRO, France
McDuffie, S.M.	Department of Energy, United States of America
Petersen, M.	United States Geological Survey, United States of America
Renault, P.	Swissnuclear, Switzerland
Romeo, R.	University of Urbino, Italy
Sánchez Cabañero, J.G.	Nuclear Safety Council, Spain
Schmitt, T.	TÜV SÜD, Germany
Seber, D.	Nuclear Regulatory Commission, United States of America
Senfaute, G.	Électricité de France, France
Serva, L.	Private consultant, Italy
Somerville, P.G.	AECOM, United States of America

Tran, M.T.	Vietnam Academy of Science and Technology, Viet Nam
Varpasuo Pentti, E.J.	PVA Engineering Services, Finland
Wu, C.J.	Nuclear Regulation Authority, Japan

Working Group Meetings

Vienna, Austria: 11–13 July 2012, 16–19 September 2013

Consultants Meetings

Tokyo, Japan: 12–16 November 2012, 06–11 July 2013

Vienna, Austria: 13–17 May 2013

Rockville, MD, USA: 02–04 December 2013

IAEA
International Atomic Energy Agency

No. 24

ORDERING LOCALLY

In the following countries, IAEA priced publications may be purchased from the sources listed below or from major local booksellers.

Orders for unpriced publications should be made directly to the IAEA. The contact details are given at the end of this list.

BELGIUM

Jean de Lannoy
Avenue du Roi 202, 1190 Brussels, BELGIUM
Telephone: +32 2 5384 308 • Fax: +32 2 5380 841
Email: jean.de.lannoy@euronet.be • Web site: http://www.jean-de-lannoy.be

CANADA

Renouf Publishing Co. Ltd.
22-1010 Polytek Street, Ottawa, ON K1J 9J1, CANADA
Telephone: +1 613 745 2665 • Fax: +1 643 745 7660
Email: order@renoufbooks.com • Web site: http://www.renoufbooks.com

Bernan Associates
4501 Forbes Blvd., Suite 200, Lanham, MD 20706-4391, USA
Telephone: +1 800 865 3457 • Fax: +1 800 865 3450
Email: orders@bernan.com • Web site: http://www.bernan.com

CZECH REPUBLIC

Suweco CZ, s.r.o.
SESTUPNÁ 153/11, 162 00 Prague 6, CZECH REPUBLIC
Telephone: +420 242 459 205 • Fax: +420 284 821 646
Email: nakup@suweco.cz • Web site: http://www.suweco.cz

FRANCE

Form-Edit
5 rue Janssen, PO Box 25, 75921 Paris CEDEX, FRANCE
Telephone: +33 1 42 01 49 49 • Fax: +33 1 42 01 90 90
Email: fabien.boucard@formedit.fr • Web site: http://www.formedit.fr

Lavoisier SAS
14 rue de Provigny, 94236 Cachan CEDEX, FRANCE
Telephone: +33 1 47 40 67 00 • Fax: +33 1 47 40 67 02
Email: livres@lavoisier.fr • Web site: http://www.lavoisier.fr

L'Appel du livre
99 rue de Charonne, 75011 Paris, FRANCE
Telephone: +33 1 43 07 43 43 • Fax: +33 1 43 07 50 80
Email: livres@appeldulivre.fr • Web site: http://www.appeldulivre.fr

GERMANY

Goethe Buchhandlung Teubig GmbH
Schweitzer Fachinformationen
Willstätterstrasse 15, 40549 Düsseldorf, GERMANY
Telephone: +49 (0) 211 49 874 015 • Fax: +49 (0) 211 49 874 28
Email: kundenbetreuung.goethe@schweitzer-online.de • Web site: http://www.goethebuch.de

HUNGARY

Librotrade Ltd., Book Import

Pesti ut 237. 1173 Budapest, HUNGARY
Telephone: +36 1 254-0-269 • Fax: +36 1 254-0-274
Email: books@librotrade.hu • Web site: http://www.librotrade.hu

INDIA

Allied Publishers

1st Floor, Dubash House, 15, J.N. Heredi Marg, Ballard Estate, Mumbai 400001, INDIA
Telephone: +91 22 4212 6930/31/69 • Fax: +91 22 2261 7928
Email: alliedpl@vsnl.com • Web site: http://www.alliedpublishers.com

Bookwell

3/79 Nirankari, Delhi 110009, INDIA
Telephone: +91 11 2760 1283/4536
Email: bkwell@nde.vsnl.net.in • Web site: http://www.bookwellindia.com

ITALY

Libreria Scientifica "AEIOU"

Via Vincenzo Maria Coronelli 6, 20146 Milan, ITALY
Telephone: +39 02 48 95 45 52 • Fax: +39 02 48 95 45 48
Email: info@libreriaaeiou.eu • Web site: http://www.libreriaaeiou.eu

JAPAN

Maruzen-Yushodo Co., Ltd.

10-10, Yotsuyasakamachi, Shinjuku-ku, Tokyo 160-0002, JAPAN
Telephone: +81 3 4335 9312 • Fax: +81 3 4335 9364
Email: bookimport@maruzen.co.jp • Web site: http://maruzen.co.jp

RUSSIAN FEDERATION

Scientific and Engineering Centre for Nuclear and Radiation Safety

107140, Moscow, Malaya Krasnoselskaya st. 2/8, bld. 5, RUSSIAN FEDERATION
Telephone: +7 499 264 00 03 • Fax: +7 499 264 28 59
Email: secnrs@secnrs.ru • Web site: http://www.secnrs.ru

UNITED STATES OF AMERICA

Bernan Associates

4501 Forbes Blvd., Suite 200, Lanham, MD 20706-4391, USA
Telephone: +1 800 865 3457 • Fax: +1 800 865 3450
Email: orders@bernan.com • Web site: http://www.bernan.com

Renouf Publishing Co. Ltd.

812 Proctor Avenue, Ogdensburg, NY 13669-2205, USA
Telephone: +1 888 551 7470 • Fax: +1 888 551 7471
Email: orders@renoufbooks.com • Web site: http://www.renoufbooks.com

Orders for both priced and unpriced publications may be addressed directly to:

IAEA Publishing Section, Marketing and Sales Unit
International Atomic Energy Agency
Vienna International Centre, PO Box 100, 1400 Vienna, Austria
Telephone: +43 1 2600 22529 or 22530 • Fax: +43 1 2600 29302
Email: sales.publications@iaea.org • Web site: http://www.iaea.org/books

16-11751

IAEA
International Atomic Energy Agency

RELATED PUBLICATIONS

FUNDAMENTAL SAFETY PRINCIPLES
IAEA Safety Standards Series No. SF-1
STI/PUB/1273 (21 pp.; 2006)
ISBN 92–0–110706–4 Price: €25.00

SITE EVALUATION FOR NUCLEAR INSTALLATIONS
IAEA Safety Standards Series No. NS-R-3 (Rev. 1)
STI/PUB/1709 (27 pp.; 2016)
ISBN 978-92-0-106515-5 Price: €35.00

SEISMIC HAZARDS IN SITE EVALUATION FOR NUCLEAR INSTALLATIONS
IAEA Safety Standards Series No. SSG-9
STI/PUB/1448 (56 pp.; 2010)
ISBN 978-92-0-102910-2) Price: €29.00

GROUND MOTION SIMULATION BASED ON FAULT RUPTURE MODELLING FOR SEISMIC HAZARD ASSESSMENT IN SITE EVALUATION FOR NUCLEAR INSTALLATIONS
Safety Reports Series No. 85
STI/PUB/1689 (126 pp.; 2015)
ISBN 978-92-0-102315-5 Price: €59.00

THE CONTRIBUTION OF PALAEOSEISMOLOGY TO SEISMIC HAZARD ASSESSMENT IN SITE EVALUATION FOR NUCLEAR INSTALLATIONS
IAEA-TECDOC-1767 (2015)
ISBN 978-92-0-105415-9 Price: €18.00

The main purpose of this report is to provide guidance for addressing the seismic hazard from diffuse seismicity zones to nuclear installations in a manner consistent with internationally recognized practices. This report may be used as a reference by regulatory organizations and by organizations responsible for the evaluation of seismic hazards for nuclear installations. The report provides definitions, phases of tasks and priorities in accordance with specific plant conditions, and a common and integrated technical framework for acceptance criteria and capacity evaluation.

INTERNATIONAL ATOMIC ENERGY AGENCY
VIENNA
ISBN 978–92–0–101716–1
ISSN 1020–6450